

Holographic Fluctuation-Dissipation Relations in Finite Density Systems

Shivam K. Sharma

International Centre for Theoretical Sciences (ICTS-TIFR)

Tata Institute of Fundamental Research, Shivakote, Hesarahatta Hobli, Bengaluru 560089, India.

E-mail: shivam.sharma@icts.res.in

ABSTRACT: Using real-time holography, we investigate fluctuation-dissipation relations in holographic systems at finite density. In the bulk, it corresponds to the study of scattering of charged scalar field against a charged black hole background and derives an exterior field theory outside the AdS Reissner-Nordström black hole. This theory captures dissipation (from infalling Quasi-normal modes) and fluctuations (from Hawking radiation). Here, we also develop a Witten diagrammatic framework for computing n -point functions for interacting charged scalars. From the boundary perspective, it gives real-time correlations of the dual CFT held at finite temperature and finite chemical potential. Our results yield (non)-linear holographic fluctuation-dissipation relations at finite density, which are shown to recover the correct behaviour in the zero-density limit.

KEYWORDS: Fluctuation-Dissipation relation, gravitational Schwinger-Keldysh, Exterior field theory

Contents

1	Introduction	1
2	RNSK geometry	4
3	Self-interacting complex scalar in RNSK	6
3.1	Free complex scalar	7
3.2	Interacting complex scalar	9
4	On-shell action & Exterior diagrammatics	10
4.1	Feynman Rules for Exterior diagrammatics	12
4.2	Contact & Exchange terms	14
5	The Gradient Expansion	16
5.1	On-shell action in gradient expansion	19
6	Holographic FDRs at finite density	20
7	Discussion	22
A	CPT action	23
B	Bulk-Bulk propagators in the RNSK geometry	24
C	Discontinuities on the RNSK geometry	28
D	On-shell action for $\Phi ^4$ theory	29
E	Explicit terms of quartic on-shell action $S_{(4)}$	32

1 Introduction

Thermal systems are present throughout physics, from everyday objects like a cup of coffee to exotic objects like black holes. The behaviour of these systems is governed by various constraints on observable quantities. A key example is the *Fluctuation-Dissipation Theorem* (FDT), which fundamentally links the strength of fluctuations to the dissipation coefficient.

A simple illustration of this can be found in Brownian motion. The dynamics of a Brownian particle is described by the Langevin's equation:

$$\ddot{q} + \gamma \dot{q} = f \eta(t) , \tag{1.1}$$

where γ is the damping coefficient, η denotes noise and f measures fluctuation strength. The relationship between these coefficients, as given by FDT, is

$$\frac{2}{\beta}\gamma = f . \quad (1.2)$$

The origin of FDT lies in the thermal nature of the bath [1]. This theorem, though powerful, is also very intuitive because the mechanisms causing dissipation are inherently linked to the fluctuations observed. A common classical argument is that the thermal fluctuations causing noise in the bath are also responsible for dissipation. In Brownian motion, for instance, random kicks from the environment not only hinder the particle's motion but also simultaneously generate noise. Then the FDT precisely asserts that, on average, the random kicks from the fluctuating force balance out the energy lost through dissipation.

Another way to understand FDTs is by considering the role of Kubo-Martin-Schwinger (KMS) conditions [2, 3] governing bath correlators. These conditions emerge from the thermal density matrix ($\hat{\rho} = e^{-\beta H}$) and define the relationships between different correlators. The 2-point KMS condition, for instance, naturally gives rise to linear FDT (see eq. (1.2)) in high-temperature limit. On the other hand, non-linear FDTs [4] arise from higher-point KMS conditions, often supplemented by additional principles like time-reversibility. A comprehensive treatment of non-linear FDTs (e.g. using non-linear Langevin's equation) via effective OTO dynamics can be found in [5–8]. A holographic discussion of non-linear Langevin theory and corresponding non-linear FDTs can be obtained in [9].

The derivation of non-linear FDTs in field theory poses significant challenges, largely due to the reliance on perturbative techniques. Holography, however, offers a powerful alternative for theories where such methods break down. The analysis of fluctuations and dissipation requires the adoption of real-time formalism of holography. Real-time holography has a rich history, starting with the work of Son-Starinets [10, 11] and Skenderis-VanRees [12, 13], each with its own limitations. To address these gaps, the authors, in [14], proposed *grSK geometry*– a gravitational counterpart to the Schwinger-Keldysh (real-time) formalism in QFT. The grSK prescription has been fruitful though its derivation is still not available.

The authors in [15], for the first time, derived non-linear FDTs within a field-theoretic setup by integrating out bath degrees of freedom. This was done with the grSK geometry via studying the physics of Hawking radiation and its interaction with the ingoing modes. For instance, they considered a particular non-linear generalization of Langevin's equation:

$$(-K\partial_t^2 + D\nabla^2 + \gamma\partial_t)\Phi + \sum_{k=1}^{n-1} \frac{\eta^k}{k!} (\theta_k + \bar{\theta}_k\partial_t)\Phi^{n-k} = f\eta , \quad (1.3)$$

and obtained the following non-linear FDTs

$$\frac{2}{\beta}\bar{\theta}_k + \theta_{k+1} + \frac{1}{4}\theta_{k-1} = 0 . \quad (1.4)$$

Here, it is important to highlight that obtaining non-linear FDTs crucially requires an understanding of the interactions in the bulk. From the bulk perspective, it amounts to studying the scattering processes against black holes in the presence of Hawking radiation. Recently in

[16, 17], a field-theoretic description has been constructed to study these scattering processes against neutral black holes. By *field-theoretic*, we refer to a diagrammatic understanding of scattering with Feynman rules to calculate the scattering amplitudes. Before discussing this field theory, let us outline some of its salient features:

- *Dissipation*: It accounts for the effects of particles falling into the black hole.
- *Fluctuations*: It incorporates thermal fluctuations caused by Hawking radiation.
- *Exterior nature*: The field theory is restricted to the region outside the black hole, as the interior remains inaccessible.

The approach involves treating the exterior field theory as an open system, with the black hole as the environment. Such systems are described by the grSK geometry¹, is constructed by connecting the two copies of the black hole exterior along their future horizons. The grSK prescription has undergone rigorous consistency checks and accurately captures the physics of Hawking radiation in various scenarios, including scalar fields, fermionic fields, gauge fields, and linearized gravity [9, 15, 19–29]. It has also been extended to cases involving chemical potentials [30, 31].²

Our goal in this note is to address the problem of scattering in case of a charged black hole. For instance, we ask: Does the existence of exterior field theory extend to charged black holes? To answer this question, we consider an interacting complex scalar field in the Reissner-Nordström black hole (RN-AdS) background. The answer suggests the existence of a field theory living outside of the outermost horizon of a charged black hole. This has been achieved by gravitational Schwinger-Keldysh formalism for charged black holes, known as *RNSK geometry* [30], which we will review in this note.

This exterior field theory captures both dissipation (due to infalling modes) and fluctuations (corresponding to Hawking radiation). Here, we develop a framework for computing n-point functions for interacting charged scalars. From the boundary perspective, it gives real-time correlations of the dual CFT held at finite temperature and finite chemical potential. Finite-density systems exhibit less understood properties of matter, such as high- T_c superconductors and non-Fermi liquids. Over the past two decades, progress has been made using the AdS/CFT correspondence to study these systems [33].

Using this exterior field theory, we want to answer whether non-linear *fluctuation-dissipation relations* (FDRs) exist for holographic systems at finite density. To do this, we will closely follow [15] where authors have evaluated non-linear FDRs by probing real scalar field in a neutral black hole at the level of contact interactions. The only major difference would be that this our probe is charged along with a charged black hole. We will keep our focus to contact interaction in this note, however the whole analysis can be generalized to the arbitrary order in coupling constant using Feynman diagrammatics.

We conclude this introduction by summarizing the key findings of this article:

¹For more details on the SK formalism and grSK geometry, see [18]

²For gravitational dual of the deformed SK contour, see [32].

- We derived the non-linear fluctuation-dissipation relation at finite density and verified its consistency in the zero-density limit.
- We constructed an exterior field theory for interacting Hawking radiation against charged black holes and developed Witten diagrammatics to analyze scattering processes.

Outline of the article

In this article, we begin with a discussion of the motivation and a review of the fluctuation-dissipation theorem, including the role of exterior field theory in describing black hole scattering. In §2, we outline the RNSK geometry and examine CPT action on fields. In §3, we solve the dynamics of a complex scalar in the RNSK geometry perturbatively. §4 introduces the Feynman diagrammatic for exterior field theory and lists relevant Witten diagrams for four- and six-point functions. In §5, we construct the SK generating functional in a gradient and small charge expansion. §6 presents (non)-linear fluctuation-dissipation relations at finite density, verifying their zero-density limit. Finally, §7 summarizes the results and suggests future directions, with appendices providing explicit calculations omitted from the main text.

2 RNSK geometry

In this section, we will briefly review the gravitational dual of Schwinger-Keldysh formalism in the context of charged black holes, i.e. *RNSK geometry*. Once we have this geometry, we will describe the CPT isometry (dual to CPT transformations on the boundary) which converts an ingoing solution to an outgoing solution.

Let us start with the Reissner–Nordström (RN) black brane solution in AdS_{d+1} in ingoing Eddington–Finkelstein coordinates and a *mock tortoise coordinate*, ζ :

$$ds^2 = -r^2 f dv^2 + i\beta r^2 f dv d\zeta + r^2 dx_{d-1}^2, \quad \mathcal{A}_M dx^M = -\mu \left(\frac{r_+}{r}\right)^{d-2} dv, \quad (2.1)$$

where f is the emblackening factor of the RN–AdS black brane, β is its inverse Hawking temperature, r_+ is its outer horizon radius, and μ is its chemical potential.³ These quantities can also be given in terms of the mass parameter M and the charge parameter Q of the black brane as,

$$f(r) \equiv 1 + \frac{Q^2}{r^{2d-2}} - \frac{M}{r^d}, \quad \frac{1}{\beta} \equiv \frac{dr_+}{4\pi} \left(1 - \frac{(d-2)Q^2}{dr_+^{2d-2}}\right), \quad \mu \equiv \frac{gQ}{r_+^{d-2}} \left[\frac{d-1}{2(d-2)}\right]^{\frac{1}{2}}, \quad (2.2)$$

where g represents the gauge coupling constant in the Einstein-Maxwell bulk action, given by,

$$\frac{1}{2\kappa^2} \int d^{d+1}x \sqrt{-g} \left[\mathcal{R} + d(d-1) - \frac{1}{g^2} \mathcal{F}_{MN} \mathcal{F}^{MN} \right], \quad (2.3)$$

where we have set the AdS radius to unity ($l_{\text{AdS}} = 1$).

³For an alternative description of the geometry in terms of orthonormal 1-forms, see [30].

The mock tortoise coordinate ζ is related to the standard radial coordinate r via the following differential equation,

$$\frac{dr}{d\zeta} = \frac{i\beta}{2} r^2 f(r). \quad (2.4)$$

The differential equation above then normalises ζ such that it has a unit jump across the logarithmic branch cut and $\zeta(r = \infty + i\varepsilon) = 0$ can be taken without any loss of generality. This condition along with the above differential equation then uniquely defines ζ everywhere in the neighbourhood of $r \in [r_+, \infty)$ (see Fig. 1).

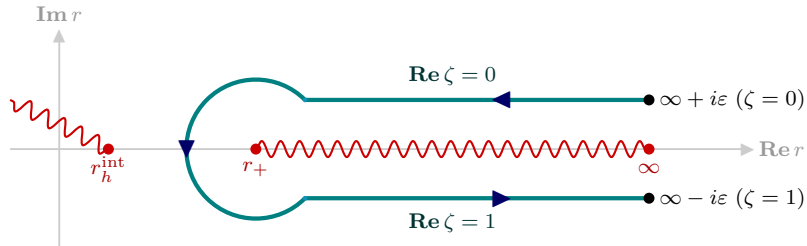


Figure 1: The radial contour drawn on the complex r plane, at fixed v . The locations of the two boundaries and the two horizons have been indicated.

We define the RNSK geometry as one constructed by taking the RN–AdS exterior and replacing the radial interval extending from the outer horizon to infinity by a doubled contour, as indicated in Fig. 1.

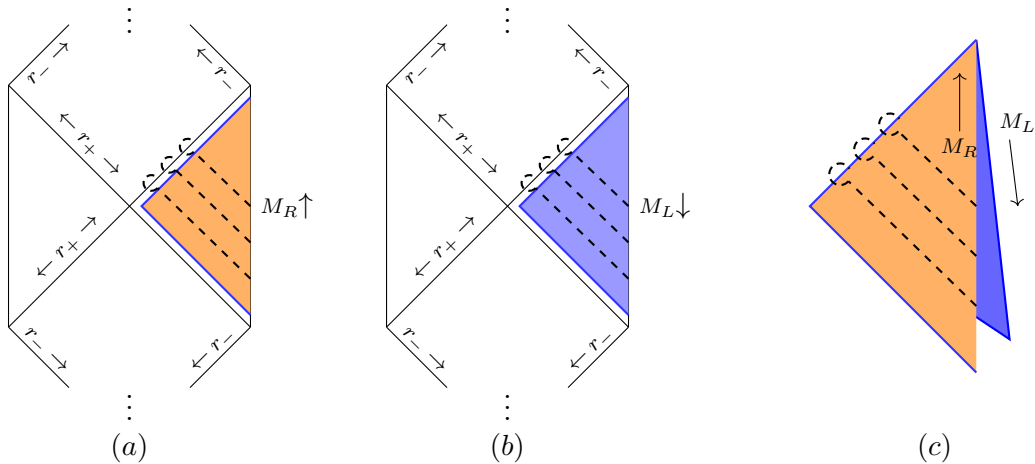


Figure 2: Schematic construction of RNSK geometry: Figures (a) and (b) show two copies of RN–AdS respectively. Figure (c) represents the RNSK geometry with the black dashed lines denoting the fixed v contours shown in Fig. 1.

We then obtain a geometry with two copies of RN–AdS exteriors smoothly stitched together by an ‘outer-horizon cap’ region. This spacetime requires one further identification — each radi-

ally constant slice must meet at the future turning point. Using sections of the Penrose diagram, the following figure (Fig. 2) schematically describes the construction of RNSK geometry.

Now that we have elaborated on the RNSK geometry and its associated notation, let us answer the following question: Given the ingoing modes, how do we construct the outgoing Hawking modes? The idea is to make use of *CPT* symmetry of the boundary CFT which acts as,

$$v \longmapsto -v, \quad \mathbf{x} \longmapsto -\mathbf{x}, \quad (2.5)$$

in addition to a charge conjugation. The implementation of this boundary CPT symmetry on the bulk fields can be done by using standard AdS/CFT rules. The detailed construction of implementation of this boundary CPT symmetry, onto the bulk is given in [30]. In particular, it was shown that boundary *CPT* transformation as an automorphism of the RN–AdS principle bundle in the bulk.

Here, we will only present the answer for a complex field of charge q :

$$\Phi_q^{\text{in}}(\zeta, k) \longmapsto e^{-\beta k^0 \zeta} e^{\beta \mu_q \Theta} \Phi_{-q}^{\text{in}}(\zeta, -k) \equiv \Phi_q^{\text{out}}(\zeta, k), \quad (2.6)$$

where we have defined

$$\mu_q \equiv \mu q, \quad \Theta(\zeta) \equiv -\frac{1}{\mu} \int_0^\zeta d\zeta' \mathcal{A}_v(\zeta') = \int_0^\zeta d\zeta' \left(\frac{r_+}{r}\right)^{d-2}. \quad (2.7)$$

The prefactor in the exponent shows that this map takes ingoing solutions that are analytic in r to outgoing solutions which exhibit branch cuts.

We end this section with a summary of how the quantities that we have introduced behave as they traverse the horizon cap. As noted before, the mock tortoise coordinate ζ has a unit jump when it encircles $r = r_+$. Noting that the gauge field \mathcal{A}_v has the value $-\mu$ at the horizon, we see that the jump in $e^{\beta \mu_q \Theta}$ is the fugacity of the boundary theory. To see, recall that there is no $\sqrt{-g}$ in the integrand in expression for Θ . So, Θ suffers a discontinuity of unity around the horizon despite \mathcal{A}_v being analytic on full grSK contour. Thus, the fugacity can be seen by evaluating different boundary limits as shown below

$$\lim_{\zeta \rightarrow 0} e^{\beta \mu_q \Theta} = 1, \quad \lim_{\zeta \rightarrow 1} e^{\beta \mu_q \Theta} = e^{\beta \mu_q}. \quad (2.8)$$

3 Self-interacting complex scalar in RNSK

In this section, we will consider an interacting charged scalar field Φ in a charged black hole background (RNSK geometry). As an illustrative example, we will only consider a massless complex scalar field interacting via quartic term⁴

$$S = - \oint d\zeta d^d x \sqrt{-g} \left[|D_M \Phi|^2 + \frac{\lambda}{2!2!} |\Phi|^4 \right], \quad \text{with } D_M \equiv \nabla_M - iq \mathcal{A}_M. \quad (3.1)$$

⁴This is chosen for simplicity, however, the whole analysis can be easily generalised to the $|\Phi|^n$ interaction.

where q and λ are the charge and the interaction parameter of the field respectively. Varying the above action, we obtain the equation of motion (EOM) for Φ :

$$D_M D^M \Phi = \frac{\lambda}{2!} \Phi |\Phi|^2 . \quad (3.2)$$

Before delving into the full dynamics and their implications, we will begin by examining the free part. Specifically, we will first describe the propagation of the scalar field Φ in the RNSK geometry, excluding interaction terms. This approach will also allow us to establish the necessary notation for subsequent sections. Later in this section, and the following one, we will use this established notation even with the interactions.

3.1 Free complex scalar

Let us begin with the linear part of the EOM (free Klein-Gordon equation) and solve it first. Later we will correct this by adding non-linear terms in the Klein-Gordon (KG) equation and solve it by using the Green's function.

The field equation for a free complex scalar field Φ is given as

$$D_M D^M \Phi = 0 , \quad \text{where} \quad D_M = \partial_M - iq \mathcal{A}_M . \quad (3.3)$$

After writing the EOM, we now turn to the solutions of this equation. As far as solutions are concerned, we will find it convenient to work in momentum space. Thus, passing into the momentum space

$$\Phi(\zeta, v, \mathbf{x}) = \int \frac{d^d k}{(2\pi)^d} \Phi(\zeta, k) e^{-ik^0 v + i\mathbf{k} \cdot \mathbf{x}} , \quad (3.4)$$

we find that the EOM can be explicitly written as

$$\begin{aligned} \frac{d}{d\zeta} \left[r^{d-1} \frac{d\Phi}{d\zeta} \right] + \frac{\beta k^0}{2} \left[r^{d-1} \frac{d\Phi}{d\zeta} + \frac{d}{d\zeta} \left(r^{d-1} \Phi \right) \right] + r^{d-1} f \left(\frac{\beta \mathbf{k}}{2} \right)^2 \Phi \\ + \frac{\beta q}{2} \left[r^{d-1} \mathcal{A}_v \frac{d\Phi}{d\zeta} + \frac{d}{d\zeta} \left(r^{d-1} \mathcal{A}_v \Phi \right) \right] = 0 . \end{aligned} \quad (3.5)$$

Since the equation of motion is a second-order ODE, the general solution is determined by two linearly independent solutions. We represent the solution using the ingoing and outgoing solutions, which are related by the CPT isometry, given in Eq. (2.6). The explicit action of this CPT transformation on the field equations is presented in Appendix A.

Thus, the free solution in terms of ingoing G^{in} and outgoing G^{out} boundary-bulk Green's function⁵, is

$$\Phi(\zeta, k) = -G^{\text{in}}(\zeta, k) J_{\bar{F}}(k) + e^{\beta(k^0 - \mu_q)} G^{\text{out}}(\zeta, k) J_{\bar{F}}(k) , \quad (3.6)$$

with the following ingoing and outgoing Green's function relationship

$$G_q^{\text{out}}(\zeta, k) = e^{-\beta k^0 \zeta} e^{\beta \mu_q \Theta} G_{-q}^{\text{in}}(\zeta, -k) , \quad (3.7)$$

⁵The approach involving ingoing and outgoing Green's functions was first investigated in [11] and subsequently elaborated upon for the grSK geometry in [9, 15].

where we have written the boundary sources in *Future-Past* (FP) basis, defined as

$$J_{\bar{F}} = -[1 + n_k] J_R + n_k J_L , \quad J_{\bar{F}} = -n_k [J_R - J_L] , \quad (3.8)$$

where n_k is the Bose-Einstein factor given by

$$n_k = \frac{1}{e^{\beta(k^0 - \mu_q)} - 1} . \quad (3.9)$$

From the relation in Eq. (3.7), it is clear that the ingoing solution is sufficient to construct the general solution. To solve for the ingoing Green's function, two boundary conditions must be supplied: (1) it must be regular at the horizon, and (2) it is normalized to unity at the boundary. These conditions are explicitly stated as:

$$\left. \frac{dG^{\text{in}}}{d\zeta} \right|_{r_+} = 0 , \quad \lim_{r \rightarrow \infty} G^{\text{in}} = 1 . \quad (3.10)$$

We will later find it convenient to write the above solution in the *right-left* (RL) basis of the sources as

$$\Phi(\zeta, k) \equiv g_R(\zeta, k) J_R(k) - g_L(\zeta, k) J_L(k) , \quad (3.11)$$

where $g_{R,L}$ denote the boundary-to-bulk Green's functions from the right and left AdS boundaries respectively, which in terms of the ingoing and the outgoing Green's functions take the form

$$\begin{aligned} g_R(\zeta, k) &\equiv (1 + n_k) [G^{\text{in}}(\zeta, k) - G^{\text{out}}(\zeta, k)] , \\ g_L(\zeta, k) &\equiv n_k [G^{\text{in}}(\zeta, k) - e^{\beta(k^0 - \mu_q)} G^{\text{out}}(\zeta, k)] . \end{aligned} \quad (3.12)$$

As it is clear from the name, the boundary conditions for these Green's functions are

$$\lim_{\zeta \rightarrow 0} g_R(\zeta, k) = 0 , \quad \lim_{\zeta \rightarrow 0} g_L(\zeta, k) = -1 , \quad (3.13)$$

and

$$\lim_{\zeta \rightarrow 1} g_R(\zeta, k) = 1 , \quad \lim_{\zeta \rightarrow 1} g_L(\zeta, k) = 0 . \quad (3.14)$$

To conclude the free Klein-Gordon equation discussion, we also provide the general solution for the free conjugate field $\bar{\Phi}$. Since the analysis for the conjugate field closely mirrors that of the field itself, we will not repeat the steps but directly present the results and move to the interactions.

The free solution for the complex-conjugate scalar field is

$$\bar{\Phi}(\zeta, k) = -\bar{G}^{\text{in}}(\zeta, k) \bar{J}_{\bar{F}}(k) + e^{\beta(k^0 + \mu_q)} \bar{G}^{\text{out}}(\zeta, k) \bar{J}_{\bar{F}}(k) , \quad (3.15)$$

with the CPT isometry relates these two Green's functions in the following manner

$$\bar{G}_q^{\text{out}}(\zeta, k) = e^{-\beta k^0 \zeta} e^{-\beta \mu_q \Theta} \bar{G}_{-q}^{\text{in}}(\zeta, -k) , \quad (3.16)$$

where we have defined the Future-Past conjugate sources as

$$\bar{J}_{\bar{F}} = -[1 + \bar{n}_k] \bar{J}_R + \bar{n}_k \bar{J}_L , \quad \bar{J}_{\bar{F}} = -\bar{n}_k [\bar{J}_R - \bar{J}_L] , \quad (3.17)$$

where \bar{n}_k is the Bose-Einstein factor given by

$$\bar{n}_k = \frac{1}{e^{\beta(k^0 + \mu_q)} - 1} . \quad (3.18)$$

In the right-left basis of the conjugate sources

$$\bar{\Phi}(\zeta, k) \equiv \bar{g}_R(\zeta, k) \bar{J}_R(k) - \bar{g}_L(\zeta, k) \bar{J}_L(k) , \quad (3.19)$$

where $\bar{g}_{R,L}$ denote the boundary-to-bulk conjugate Green's functions from the right and left AdS boundaries for the complex field, which in terms of the ingoing and the outgoing conjugate Green's functions take the form

$$\begin{aligned} \bar{g}_R(\zeta, k) &\equiv (1 + \bar{n}_k) [\bar{G}^{\text{in}}(\zeta, k) - \bar{G}^{\text{out}}(\zeta, k)] , \\ \bar{g}_L(\zeta, k) &\equiv \bar{n}_k [\bar{G}^{\text{in}}(\zeta, k) - e^{\beta(k^0 + \mu_q)} \bar{G}^{\text{out}}(\zeta, k)] . \end{aligned} \quad (3.20)$$

Again, the boundary conditions for these conjugate Green's functions are

$$\lim_{\zeta \rightarrow 0} \bar{g}_R(\zeta, k) = 0 , \quad \lim_{\zeta \rightarrow 0} \bar{g}_L(\zeta, k) = -1 , \quad (3.21)$$

and

$$\lim_{\zeta \rightarrow 1} \bar{g}_R(\zeta, k) = 1 , \quad \lim_{\zeta \rightarrow 1} \bar{g}_L(\zeta, k) = 0 . \quad (3.22)$$

3.2 Interacting complex scalar

Now that we have worked through the free Klein-Gordon equation and its solutions, we can move on to interactions. In this part, we will consider the full quartic theory and use the Green function method in the bulk to determine the interactive portion of the solution.

For completeness, we once again write the full Klein-Gordon field equation as

$$D_M D^M \Phi = \frac{\lambda}{2!} \Phi |\Phi|^2 . \quad (3.23)$$

We will solve this field equation perturbatively in the coupling constant λ by expanding the Φ as

$$\Phi = \sum_{i=0}^{\infty} \lambda^i \Phi_{(i)} = \Phi_{(0)} + \lambda \Phi_{(1)} + \lambda^2 \Phi_{(2)} \dots , \quad (3.24)$$

under the double-Dirichlet boundary conditions (same as for free theory), given by

$$\lim_{\zeta \rightarrow 0,1} \Phi_{(0)} = J_{L,R} , \quad \lim_{\zeta \rightarrow 0,1} \Phi_{(i)} = 0 \quad \forall \quad i > 1 , \quad (3.25)$$

where $J_{L,R}$ are the left and the right boundary sources respectively. The boundary conditions above are *doubled* versions of the standard conditions in AdS/CFT, modified specifically to fit the Schwinger-Keldysh formalism. The leading-order solution $\Phi_{(0)}$ is just the free solution that we have already obtained in Eq. (3.6). Regarding the boundary conditions, $\Phi_{(0)}$ satisfies the GKPW conditions, while all higher-order corrections should vanish at both boundaries consistent with Eq. (3.25).

To find the higher-order solution, we use the *bulk-to-bulk* Green's function. This function should vanish at both boundaries and is therefore termed *binormalisable*. The binormalisable bulk-to-bulk Green's function \mathbb{G} satisfies:

$$D_M D^M \mathbb{G}(\zeta|\zeta', k) = \frac{\delta(\zeta - \zeta')}{\sqrt{-g}}, \quad (3.26)$$

where $\delta(\zeta - \zeta')$ is the radial delta function on the RNSK contour. The above differential equation should be solved with the following boundary conditions

$$\lim_{\zeta \rightarrow 0} \mathbb{G}(\zeta|\zeta', k) = \lim_{\zeta \rightarrow 1} \mathbb{G}(\zeta|\zeta', k) = 0. \quad (3.27)$$

The explicit expression for the bulk-to-bulk Green's function is derived in the Appendix B and given as

$$\mathbb{G}(\zeta|\zeta', k) = \frac{e^{\beta k^0 \zeta' - \beta \mu_q \Theta(\zeta')}}{(1 + n_k)} \left(\frac{\Theta(\zeta > \zeta') g_L(\zeta, k) g_R(\zeta', k) + \Theta(\zeta < \zeta') g_R(\zeta, k) g_L(\zeta', k)}{[K_q^{\text{in}}(k) - K_{-q}^{\text{in}}(-k)]} \right), \quad (3.28)$$

where Θ is the radial Heavyside step function on the RNSK contour.

With the help of the bulk-to-bulk Green's function, the remaining higher-order terms can be written as:

$$\Phi_{(i)}(\zeta, k) = \oint_{\zeta'} \mathbb{G}(\zeta|\zeta', k) \mathbb{J}_{(i)}(\zeta', k), \quad \text{with} \quad \oint_{\zeta} \equiv \oint d\zeta \sqrt{-g}, \quad (3.29)$$

where $\mathbb{J}_{(i)}$ are bulk sources for i -th order term in the solution. The first few terms of bulk sources are as follows:

$$\begin{aligned} \mathbb{J}_{(1)}(\zeta, k) &= \int \prod_{i=1}^3 \left(\frac{d^d p_i}{(2\pi)^d} \right) (2\pi)^d \delta^d \left(\sum_i^3 p_i - k \right) \frac{1}{2!} \Phi_{(0)}(\zeta, p_1) \bar{\Phi}_{(0)}(\zeta, p_2) \Phi_{(0)}(\zeta, p_3), \\ \mathbb{J}_{(2)}(\zeta, k) &= \int \prod_{i=1}^3 \left(\frac{d^d p_i}{(2\pi)^d} \right) (2\pi)^d \delta^d \left(\sum_i^3 p_i - k \right) \\ &\quad \times \left[\Phi_{(1)}(\zeta, p_1) \bar{\Phi}_{(0)}(\zeta, p_2) \Phi_{(0)}(\zeta, p_3) + \frac{1}{2!} \Phi_{(0)}(\zeta, p_1) \bar{\Phi}_{(1)}(\zeta, p_2) \Phi_{(0)}(\zeta, p_3) \right]. \end{aligned} \quad (3.30)$$

4 On-shell action & Exterior diagrammatics

In this section, we derive the on-shell action for the $|\Phi|^4$ theory in the RNSK background. Previously, in §3, we explained the method for solving the bulk field equations to arbitrary orders in the coupling constant λ . By substituting these solutions into the action, we can compute the on-shell action to any desired order in λ .⁶ Our approach, also used in [17], circumvents the need to evaluate the boundary terms in the on-shell action explicitly. It leverages the fact that the boundary value of the higher-order solution vanishes, thereby simplifying the computation.

⁶Since our analysis is limited to tree-level diagrams, we use on-shell action and tree-level influence phase interchangeably.

The bare action S_{bare} is given by

$$S_{\text{bare}} = - \oint_{\mathcal{M}} \left(|D_M \Phi|^2 + \frac{\lambda}{2!2!} |\Phi|^4 \right), \quad \text{where} \quad \oint_{\mathcal{M}} \equiv \oint d\zeta d^d x \sqrt{-g}, \quad (4.1)$$

where \mathcal{M} denotes the RNSK background. Inserting the perturbative solution into the bare action yields the *on-shell action* S_{os} in the following form:

$$S_{\text{os}} = - \int_{\partial\mathcal{M}} \Phi_{(0)} \overline{(D_A \Phi_{(0)})} + \lambda \oint_{\mathcal{M}} \left[\frac{1}{2!} (\bar{\Phi} - \bar{\Phi}_{(0)}) \Phi |\Phi|^2 - \frac{1}{2!2!} |\Phi|^4 \right], \quad (4.2)$$

where $\partial\mathcal{M}$ denotes the boundary of \mathcal{M} . Note that in deriving Eq. (4.2), we have used the equations of motion and imposed the appropriate boundary conditions to significantly simplify the expression for the on-shell action.

The on-shell action S_{os} , expanded in powers of λ , is expressed as:

$$S_{\text{os}} = S_{(2)} + \lambda S_{(4)} + \lambda^2 S_{(6)} + \dots, \quad (4.3)$$

where the subscript indicates the number of boundary sources in each term. For example, the quadratic term $S_{(2)}$, the quartic term $S_{(4)}$ and the term with six sources $S_{(6)}$ are given by:

$$\begin{aligned} S_{(2)} &= - \int_{\partial\mathcal{M}} \Phi_{(0)} \overline{(D_A \Phi_{(0)})}, \\ S_{(4)} &= - \frac{\lambda}{2!2!} \oint_{\mathcal{M}} (\bar{\Phi}_{(0)} \Phi_{(0)})^2, \\ S_{(6)} &= - \frac{\lambda^2}{2} \oint_{\mathcal{M}} \bar{\Phi}_{(0)} \Phi_{(1)} \bar{\Phi}_{(0)} \Phi_{(0)}. \end{aligned} \quad (4.4)$$

The terms above correspond to the free, contact, and single-exchange contributions at the tree level in Feynman diagrams. Within the framework of open effective field theory [15, 27], $S_{(n)}$ represents the n -point influence phase of the boundary theory.

We find it useful to express the on-shell action in the *Past-Future* (PF) basis, as shown in Eqs. (3.8) and (3.17). In this basis, the Schwinger-Keldysh collapse (unitarity) and the Kubo-Martin-Schwinger conditions (thermalicity) manifest as the vanishing of coefficients for terms involving all Future and all Past sources, respectively. Furthermore, this basis exclusively incorporates retarded/advanced propagators in the boundary correlators, ensuring the description of causal scattering processes.

The explicit computation of the on-shell action requires evaluating monodromy integrals on the RNSK contour. This involves a contour integral over the complexified radial coordinate, as illustrated in Fig. 1. The integral simplifies into a single exterior radial integral, with discontinuities arising at the horizon cap. The origin and evaluation of these discontinuities are detailed in Appendix C. Using the discontinuity formulas, the on-shell action can be expressed in terms of a single exterior radial integral, as shown in Appendix D.

To declutter the expressions, we write the terms in the on-shell action in the following way

$$S_{(2n)} = \int_{k_1, 2, \dots, 2n} \sum_{r,s=0}^n \mathcal{I}_{p,q}^{(2n)}(k_1, \dots, k_{2n}) \prod_{i=1}^p \bar{J}_{\bar{F}}(k_i) \prod_{j=1}^q J_{\bar{F}}(k_j) \prod_{l=p+1}^n \bar{J}_{\bar{F}}(k_l) \prod_{m=q+1}^n J_{\bar{F}}(k_m), \quad (4.5)$$

where we have used the following notation

$$\int_{k_1, 2, \dots, m} \equiv \int \frac{d^d k_1}{(2\pi)^d} \int \frac{d^d k_2}{(2\pi)^d} \dots \int \frac{d^d k_m}{(2\pi)^d} \delta^{(d)}(k_1 + k_2 + \dots + k_m) . \quad (4.6)$$

From this point onward, we will only present the expressions for $\mathcal{I}_{p,q}$ derived from RNSK geometry. The physical interpretation of $\mathcal{I}_{p,q}$ corresponds to a scattering process, where p and q ingoing modes with charges $-$ and $+$, respectively, scatter into $(n-p)$ and $(n-q)$ outgoing modes with charges $+$ and $-$, respectively. Although the results themselves are intricate, there is a particularly insightful way to summarize them that highlights their physical significance. We find that our findings can be concisely represented by a diagrammatic expansion governed by the Feynman rules.

4.1 Feynman Rules for Exterior diagrammatics

As discussed earlier, the explicit computation of the on-shell action in the bulk naturally gives rise to an *exterior field theory*. This theory exists outside the outermost horizon of the RN-AdS black hole. Next, we will demonstrate how this exterior field theory can be utilized to compute boundary correlation functions. The key idea is to define Feynman diagrammatic rules for the exterior theory and then apply these rules to compute the on-shell action (or boundary generating functional).

Below, we outline the diagrammatic rules for computing the tree-level influence phase (on-shell action). The conventions for momentum flow are as follows: in boundary-to-bulk propagators, momentum flows from the boundary to the bulk, while in bulk-to-bulk propagators, it flows from left to right.

The *boundary-to-bulk propagators* for complex scalar and its conjugate field are:

$$\begin{array}{c} \text{---} \\ | \\ \uparrow \text{ } \nabla \text{ } k \\ | \\ \bullet \text{ } r \end{array} \equiv \frac{G^{\text{in}}(r, k)}{1+n_k} J_{\bar{F}}(k) , \quad \begin{array}{c} \text{---} \\ | \\ \uparrow \text{ } \triangle \\ | \\ \bullet \text{ } r \end{array} \equiv G^{\text{out}}(r, k) J_{\bar{F}}(k) , \quad (4.7)$$

$$\begin{array}{c} \text{---} \\ | \\ \downarrow \text{ } \nabla \text{ } k \\ | \\ \bullet \text{ } r \end{array} \equiv \frac{\bar{G}^{\text{in}}(r, k)}{1+\bar{n}_k} \bar{J}_{\bar{F}}(k) , \quad \begin{array}{c} \text{---} \\ | \\ \downarrow \text{ } \triangle \\ | \\ \bullet \text{ } r \end{array} \equiv \bar{G}^{\text{out}}(r, k) \bar{J}_{\bar{F}}(k) , \quad (4.8)$$

and the *bulk-to-bulk propagators* are:

$$\begin{array}{c} \bullet \\ | \\ \xrightarrow{k} \triangle \\ | \\ \bullet \end{array} \equiv -i\mathbb{G}_{\text{ret}}(r_2|r_1, k) , \quad \begin{array}{c} \bullet \\ | \\ \triangle \\ | \\ \bullet \end{array} \equiv -i\mathbb{G}_{\text{adv}}(r_2|r_1, k) . \quad (4.9)$$

where the red-colored arrow indicates the direction of charge. It is important to note that all propagators are expressed in a basis that explicitly reveals their causal properties. As a result, the causal structure of Witten diagrams will naturally emerge during their construction, thereby simplifying the understanding of scattering processes against black holes.

The final ingredient needed to construct the Witten diagrams is the set of bulk vertices. Before specifying the vertices in this exterior field theory, it is useful to first define

$$n_{\alpha,k} \equiv \frac{1}{e^{\beta(k^0 - \alpha \mu_q)} - 1}, \quad \text{and} \quad k_{12\dots m} \equiv k_1 + k_2 + \dots k_m, \quad (4.10)$$

where we note $n_{1,k} = n_k$ and $n_{-1,k} = \bar{n}_k$ and we will use these two relations interchangeably. Now, let us come to the *vertices* in this exterior field theory, given as follows:

$$= -i\lambda \frac{\bar{n}_{-k_1}}{n_{1,k_{234}}}, \quad = -i\lambda \frac{n_{-k_2}}{n_{-1,k_{134}}}, \quad (4.11)$$

and

$$= -i\lambda \frac{\bar{n}_{-k_1} \bar{n}_{-k_3}}{n_{2,k_{24}}}, \quad = -i\lambda \frac{n_{-k_2} n_{-k_4}}{n_{-2,k_{13}}}, \quad (4.12)$$

$$= -i\lambda \frac{\bar{n}_{-k_1} n_{-k_2}}{n_{0,k_{34}}}, \quad (4.13)$$

and

$$= -i\lambda \frac{\bar{n}_{-k_1} n_{-k_2} n_{-k_4}}{n_{-1,k_3}}, \quad = -i\lambda \frac{\bar{n}_{-k_1} n_{-k_2} \bar{n}_{-k_3}}{n_{1,k_4}}. \quad (4.14)$$

where one can easily see the charge conservation at the bulk vertex. For each of the vertices above, we have chosen the convention that all momenta flow into the vertex. Only these vertices contribute non-zero terms, while the rest vanish. More precisely, vertices with same legs result

in no contribution as shown below

$$= 0 = \tag{4.15}$$

Along with the above Feynman rules for propagators and vertices, to obtain the *boundary Schwinger-Keldysh generating functional* (on-shell action),⁷ we must further

1. Multiply every diagram by i .
2. Divide by the symmetry factor of the diagram.
3. The vertices are integrated over the exterior of the blackbrane, with the following radial exterior integral

$$\int_{\text{ext}} = \int_{r_+}^{r_c} dr r^{d-1} \tag{4.16}$$

where r_c is the cutoff on the radial coordinate required for holographic renormalisation [12].

Using the Feynman rules for Witten diagrams outlined above, we can calculate the boundary SK generating functional to any desired order in λ . In this note, we only present the result up to quadratic order in λ , incorporating contributions from contact and single exchange diagrams.

4.2 Contact & Exchange terms

We begin with the contact diagrams contributing to the four-point influence phase. The corresponding four-point contact term in the on-shell action is given by:

$$S_{(4)} = -\frac{\lambda}{2!2!} \int_{k_{1,2,3,4}} \oint_{\zeta} \prod_{i=1}^2 \bar{\Phi}_{(0)}(\zeta, k_i) \prod_{j=1}^2 \Phi_{(0)}(\zeta, k_j) \tag{4.17}$$

where we have taken $S_{(4)}$ from the Eq. (4.4) and written in the momentum space.

Using the solutions of the Klein-Gordon equation and performing the RNSK radial contour integral, as explained in previous sections. We obtain the on-shell action at linear order in coupling constant $S_{(4)}$, and read off $\mathcal{I}_{p,q}^{(4)}(k_1, k_2, k_3, k_4)$ as explained in the Appendix D. The diagrams contributing to the $S_{(4)}$ are:

⁷It is equal to the boundary influence phase in the large N limit.

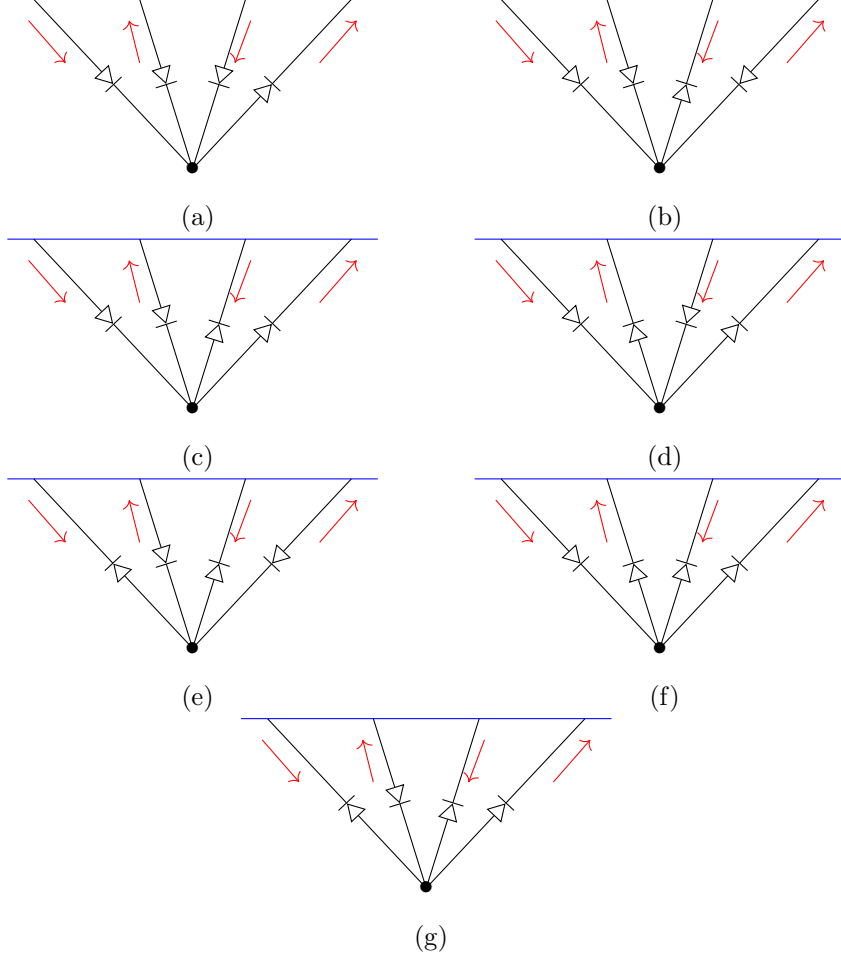


Figure 3: Witten diagrams that contribute to the four-point influence phase $S_{(4)}$.

and the terms corresponding to these diagrams are:

$$\begin{aligned}
\mathcal{I}_{2,1}^{(4)} &= -\frac{\lambda}{2} \frac{1}{n_{k_4}} \int_{\text{ext}} \bar{G}^{\text{in}}(r, k_1) G^{\text{in}}(r, k_2) \bar{G}^{\text{in}}(r, k_3) G^{\text{out}}(r, k_4) , \\
\mathcal{I}_{1,2}^{(4)} &= -\frac{\lambda}{2} \frac{1}{\bar{n}_{k_3}} \int_{\text{ext}} \bar{G}^{\text{in}}(r, k_1) G^{\text{in}}(r, k_2) \bar{G}^{\text{out}}(r, k_3) G^{\text{in}}(r, k_4) , \\
\mathcal{I}_{1,1}^{(4)} &= \lambda \frac{1}{n_{0,k_{34}}} \int_{\text{ext}} \bar{G}^{\text{in}}(r, k_1) G^{\text{in}}(r, k_2) \bar{G}^{\text{out}}(r, k_3) G^{\text{out}}(r, k_4) , \\
\mathcal{I}_{2,0}^{(4)} &= \lambda \frac{1}{n_{2,k_{24}}} \int_{\text{ext}} \bar{G}^{\text{in}}(r, k_1) G^{\text{out}}(r, k_2) \bar{G}^{\text{in}}(r, k_3) G^{\text{out}}(r, k_4) , \\
\mathcal{I}_{0,2}^{(4)} &= \lambda \frac{1}{n_{-2,k_{13}}} \int_{\text{ext}} \bar{G}^{\text{out}}(r, k_1) G^{\text{in}}(r, k_2) \bar{G}^{\text{out}}(r, k_3) G^{\text{in}}(r, k_4) , \\
\mathcal{I}_{1,0}^{(4)} &= -\frac{\lambda}{2} \frac{1}{n_{k_{234}}} \int_{\text{ext}} \bar{G}^{\text{in}}(r, k_1) G^{\text{out}}(r, k_2) \bar{G}^{\text{out}}(r, k_3) G^{\text{out}}(r, k_4) , \\
\mathcal{I}_{0,1}^{(4)} &= -\frac{\lambda}{2} \frac{1}{\bar{n}_{k_{134}}} \int_{\text{ext}} \bar{G}^{\text{out}}(r, k_1) G^{\text{in}}(r, k_2) \bar{G}^{\text{out}}(r, k_3) G^{\text{out}}(r, k_4) ,
\end{aligned} \tag{4.18}$$

where we have removed the momentum dependence in $\mathcal{I}_{p,q}^{(4)}$ to shorten the expressions.

Next, we come to the exchange diagrams contributing to the six-point influence phase. The corresponding six-point contact term in the on-shell action is given by:

$$S_{(6)} = -\frac{\lambda^2}{4} \int_{k_{1,2,3,4,5,6}} \times \oint_{\zeta, \zeta'} \bar{\Phi}_{(0)}(\zeta, k_1) \Phi_{(0)}(\zeta, k_2) \bar{\Phi}_{(0)}(\zeta, k_3) \mathbb{G}(\zeta | \zeta', k_{456}) \Phi_{(0)}(\zeta', k_4) \bar{\Phi}_{(0)}(\zeta', k_5) \Phi_{(0)}(\zeta', k_6) \quad (4.19)$$

Additional details can be found in Appendix D. Here, we illustrate a few diagrams that contribute to $S_{(6)}$, while noting that other diagrams can be similarly derived using the same Feynman rules. Below are two such examples:

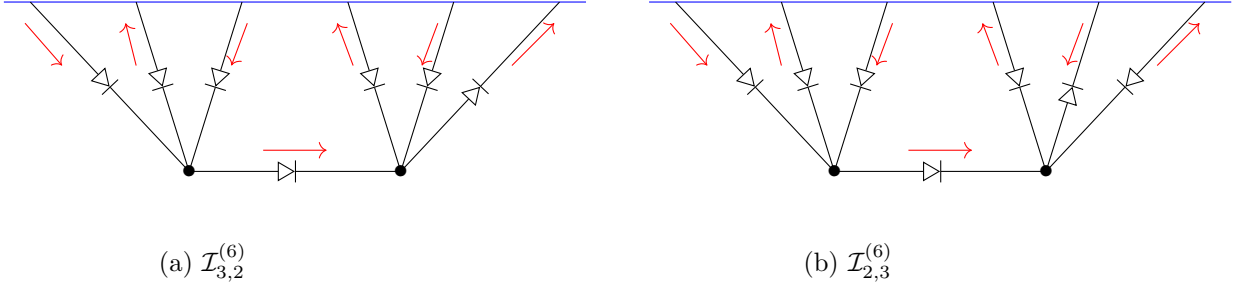


Figure 4: Two particular Witten diagrams that contribute to $S_{(6)}$.

and terms corresponding to these diagrams are:

$$\begin{aligned} \mathcal{I}_{3,2}^{(6)} &= \frac{\lambda^2}{2} \frac{1}{n_{k_6}} \int_{\text{ext}} \mathbb{G}_{\text{ret}}(r|r', k_{123}) [\bar{G}^{\text{in}}(r, k_1) G^{\text{in}}(r, k_2) \bar{G}^{\text{in}}(r, k_3) G^{\text{in}}(r', k_4) \bar{G}^{\text{in}}(r', k_5) G^{\text{out}}(r', k_6)] , \\ \mathcal{I}_{2,3}^{(6)} &= \frac{\lambda^2}{2} \frac{1}{\bar{n}_{k_5}} \int_{\text{ext}} \mathbb{G}_{\text{ret}}(r|r', k_{123}) [\bar{G}^{\text{in}}(r, k_1) G^{\text{in}}(r, k_2) \bar{G}^{\text{in}}(r, k_3) G^{\text{in}}(r', k_4) \bar{G}^{\text{out}}(r', k_5) G^{\text{in}}(r', k_6)] . \end{aligned} \quad (4.20)$$

In a similar manner, higher-point exchange diagrams contributing to the higher-point influence phase can be built using the Feynman rules described above. This concludes our analysis of exterior diagrammatics, and we now shift focus to constructing solutions explicitly within the gradient expansion.

5 The Gradient Expansion

In this section, we solve the complex Klein-Gordon equation by expressing the field in the gradient expansion. To derive the *fluctuation-dissipation relations* (FDRs), we only need to assume that the field Φ is independent of the boundary space coordinates \mathbf{x} . This is equivalent to setting its Fourier counterpart $\mathbf{k} = 0$ in momentum space. Under this assumption, the complex Klein-Gordon equation (3.23) reduces to the explicit form given below:

$$\frac{d}{d\zeta} \left[r^{d-1} \frac{d\Phi}{d\zeta} \right] + \frac{\beta k^0}{2} \left[r^{d-1} \frac{d\Phi}{d\zeta} + \frac{d}{d\zeta} (r^{d-1} \Phi) \right] - \frac{\beta \mu q}{2} \left[r r_+^{d-2} \frac{d\Phi}{d\zeta} + \frac{d}{d\zeta} (r r_+^{d-2} \Phi) \right] = 0 , \quad (5.1)$$

where we have used the explicit expression for the gauge field \mathcal{A}_v , given in Eq. (2.1).

We begin by writing the most general solution (with $\mathbf{k} = 0$) in a gradient expansion near $\omega \sim \mu_q$ as

$$\Phi = \sum_i \left(\frac{\beta(k^0 - \mu_q)}{2} \right)^i \phi_i(\zeta). \quad (5.2)$$

Upon using this expansion in the field equations (5.1), we obtain the field equations at different orders as

$$\begin{aligned} \frac{d}{d\zeta} \left[r^{d-1} \frac{d\phi_0}{d\zeta} + \beta\mu_q \left(r^{d-1} - r r_+^{d-2} \right) \phi_0 \right] &= \frac{\beta\mu_q}{2} \left(r^{d-1} - r r_+^{d-2} \right)' \phi_0, \\ \frac{d}{d\zeta} \left[r^{d-1} \frac{d\phi_1}{d\zeta} + \beta\mu_q \left(r^{d-1} - r r_+^{d-2} \right) \phi_1 + 2r^{d-1} \phi_0 \right] &= \left[r^{d-1} \right]' \phi_0 + \frac{\beta\mu_q}{2} \left[r^{d-1} - r r_+^{d-2} \right]' \phi_1, \\ \frac{d}{d\zeta} \left[r^{d-1} \frac{d\phi_2}{d\zeta} + \beta\mu_q \left(r^{d-1} - r r_+^{d-2} \right) \phi_2 + 2r^{d-1} \phi_1 \right] &= \left[r^{d-1} \right]' \phi_1 + \frac{\beta\mu_q}{2} \left[r^{d-1} - r r_+^{d-2} \right]' \phi_2, \end{aligned} \quad (5.3)$$

where $'$ denotes the derivative w.r.t ζ and the first, second and third lines represent zeroth, first and second-order field equations in the gradient expansion respectively.

We find it hard to solve these equations for arbitrary charge q . Therefore, we employ a small charge ($q \sim 0$) expansion, as outlined below

$$\phi_i = \sum_j (\beta\mu_q)^j \phi_{i,j}(\zeta). \quad (5.4)$$

As discussed in the previous sections, it suffices to evaluate the ingoing solution, since the most general solution can be constructed using the CPT isometry. To determine the ingoing boundary-to-bulk Green's function G^{in} , we will solve the field equations (5.1) under the following boundary conditions:

$$G^{\text{in}}|_{r_c} = 1, \quad \left. \frac{dG^{\text{in}}}{d\zeta} \right|_{r_+} = 0. \quad (5.5)$$

Under the assumption that ingoing Green's function G^{in} is independent of the boundary space coordinates \mathbf{x} , the G^{in} can be solved in the gradient expansion given above. Here we will only present the answer for G^{in} without going into the details of obtaining it.⁸

Thus, the ingoing boundary-to-bulk Green's function in the gradient expansion under the small charge regime as

$$G^{\text{in}} = \sum_{i,j} G_{i,j}^{\text{in}}(\zeta) \left(\frac{\beta(k^0 - \mu_q)}{2} \right)^i (\beta\mu_q)^j, \quad (5.6)$$

with the coefficients $G_{i,j}^{\text{in}}$ explicitly given below

$$\begin{aligned} G_{0,0}^{\text{in}} &= 1, & G_{0,1}^{\text{in}} &= \frac{1}{2} \mathbb{F}_2(r), & G_{1,0}^{\text{in}} &= \mathbb{F}_1(r), \\ G_{2,0}^{\text{in}} &= \int_{\zeta_c}^{\zeta} \frac{d\bar{\zeta}}{\bar{r}^{d-1}} \int_{\zeta_h}^{\bar{\zeta}} d\hat{\zeta} \left[\hat{r}^{d-1} \right]' \mathbb{F}_1(\hat{r}) - 2 \int_{\zeta_c}^{\zeta} d\bar{\zeta} \left(\mathbb{F}_1(r) - \frac{r_+^{d-1}}{r^{d-1}} \mathbb{F}_1(r_+) \right), \end{aligned} \quad (5.7)$$

⁸We follow analysis similar to that of [15] for obtaining G^{in} .

where we have defined

$$\mathbb{F}_n(r) \equiv \int_{\zeta_c}^{\zeta} d\bar{\zeta} \left[\left(\frac{r_+}{\bar{r}} \right)^{d-n} - 1 \right], \quad \zeta_h \equiv \zeta(r_+), \quad \zeta_c \equiv \zeta(r_c). \quad (5.8)$$

The \mathbb{F}_n is analytic on the radial RNSK contour as long as $n < d$. The other remaining terms are written below:

$$\begin{aligned} G_{1,1}^{\text{in}} + \int_{\zeta_c}^{\zeta} d\bar{\zeta} \left(1 - \frac{\bar{r} r_+^{d-2}}{\bar{r}^{d-1}} \right) \mathbb{F}_1(\bar{r}) + \int_{\zeta_c}^{\zeta} d\bar{\zeta} \left(\mathbb{F}_2(r) - \frac{r_+^{d-1}}{r^{d-1}} \mathbb{F}_2(r_+) \right) = \\ + \frac{1}{2} \int_{\zeta_c}^{\zeta} \frac{d\bar{\zeta}}{\bar{r}^{d-1}} \int_{\zeta_h}^{\bar{\zeta}} d\hat{\zeta} \left[\hat{r}^{d-1} \right]' \mathbb{F}_2(\hat{r}) + \frac{1}{2} \int_{\zeta_c}^{\zeta} \frac{d\bar{\zeta}}{\bar{r}^{d-1}} \int_{\zeta_h}^{\bar{\zeta}} d\hat{\zeta} \left[\hat{r}^{d-1} - \hat{r} r_+^{d-2} \right]' \mathbb{F}_1(\hat{r}), \end{aligned} \quad (5.9)$$

and

$$\begin{aligned} G_{2,1}^{\text{in}} + \int_{\zeta_c}^{\zeta} d\bar{\zeta} \left[1 - \left(\frac{r_+}{\bar{r}} \right)^{d-2} \right] G_{2,0}^{\text{in}}(\bar{r}) + 2 \int_{\zeta_c}^{\zeta} d\bar{\zeta} \left(G_{1,1}^{\text{in}}(\bar{r}) - \frac{r_+^{d-1}}{\bar{r}^{d-1}} G_{1,1}^{\text{in}}(r_+) \right) \\ = \int_{\zeta_c}^{\zeta} d\bar{\zeta} \frac{1}{\bar{r}^{d-1}} \int_{\zeta_h}^{\bar{\zeta}} d\hat{\zeta} \left[\hat{r}^{d-1} \right]' G_{1,1}^{\text{in}}(\hat{r}) + \frac{1}{2} \int_{\zeta_h}^{\bar{\zeta}} d\bar{\zeta} \frac{1}{\bar{r}^{d-1}} \int_{\zeta_h}^{\bar{\zeta}} d\hat{\zeta} \left[\hat{r}^{d-1} - \hat{r} r_+^{d-2} \right]' G_{2,0}^{\text{in}}(\hat{r}). \end{aligned} \quad (5.10)$$

Similarly, the ingoing boundary-to-bulk conjugate Green's function by replacing $q \rightarrow -q$.

We will now express the field in the gradient and charge expansion, retaining terms up to linear order. The approach involves first constructing the ingoing solution and then applying the CPT isometry to obtain the full solution up to first order in both expansions. We find it helpful to represent the solution (3.11) in the following form,

$$\Phi = G_q^{\text{in}}(r, k) \left[J_a(k) + \left(n_k + \frac{1}{2} \right) J_d(k) \right] - e^{\beta\mu_q[\Theta(\zeta)-1]} e^{-\beta k^0(\zeta-1)} G_{-q}^{\text{in}}(r, -k) n_k J_d(k), \quad (5.11)$$

where we have defined the sources in *average-difference* basis as

$$J_a \equiv \frac{1}{2} (J_R + J_L), \quad J_d \equiv J_R - J_L. \quad (5.12)$$

By expanding the solution in both parameters (k^0 and q) and using Eqs. (5.6) along with their explicit coefficients as derived above, the complete solution to leading order is given by:

$$\begin{aligned} \Phi = \left[J_a + \left(\zeta - \frac{1}{2} + \mathbb{F}_1 \right) J_d \right] + \frac{\beta k^0}{2} \left[\mathbb{F}_1 J_a - \left(\zeta(\zeta - 1) + \left[\zeta - \frac{1}{2} \right] \mathbb{F}_1 \right) J_d \right] \\ + \frac{\beta\mu_q}{2} \left[(\mathbb{F}_2 - \mathbb{F}_1) J_a + \left(\zeta(\zeta - 1) + \left[\zeta - \frac{1}{2} \right] \mathbb{F}_2 + \left(\zeta - \frac{1}{2} + \mathbb{F}_2 \right) \mathbb{F}_1 \right) J_d \right] + \dots \end{aligned} \quad (5.13)$$

Here, we have omitted the subscript indicating zeroth-order, as the context makes it clear. To conclude the discussion on gradient expansion, we provide the solution in position-space as well. This form will be significant when we evaluate the non-linear FDRs in the next section.

In position-space coordinates, the solution can be written as

$$\begin{aligned} \Phi = \left[J_a + \left(\zeta - \frac{1}{2} + \mathbb{F}_1 \right) J_d \right] + \frac{i\beta}{2} \left[\mathbb{F}_1 \partial_t J_a - \left(\zeta(\zeta - 1) + \left[\zeta - \frac{1}{2} \right] \mathbb{F}_1 \right) \partial_t J_d \right] \\ + \frac{\beta\mu_q}{2} \left[(\mathbb{F}_2 - \mathbb{F}_1) J_a + \left(\zeta(\zeta - 1) + \left[\zeta - \frac{1}{2} \right] \mathbb{F}_2 + \left(\zeta - \frac{1}{2} + \mathbb{F}_2 \right) \mathbb{F}_1 \right) J_d \right] + \dots, \end{aligned} \quad (5.14)$$

where we have replaced $k^0 \mapsto i\partial_t$ to obtain the above result.

5.1 On-shell action in gradient expansion

Using the gradient expansion solutions from Eqs. (5.13) and (5.14), we proceed to compute the on-shell action (or influence phase), starting with the quadratic (free) contribution $S_{(2)}$, given as

$$S_{(2)} = - \int d^d x \sqrt{-g} \Phi_{(0)} \left(\overline{\mathbb{D}\Phi_{(0)}} \right) \Big|_{\zeta=0}^{\zeta=1}. \quad (5.15)$$

Upon transitioning to momentum space, the on-shell action at quadratic order in the *average-difference* basis is found to be:

$$S_{(2)} = \int \frac{d^d k}{(2\pi)^d} [\mathcal{G}_{ad} \bar{J}_a(-k) J_a(k) + \mathcal{G}_{da} \bar{J}_a(-k) J_d(k) + \mathcal{G}_{dd} \bar{J}_a(-k) J_d(k)] , \quad (5.16)$$

with \mathcal{G}_{ad} , \mathcal{G}_{da} and \mathcal{G}_{dd} are the boundary Green's functions given below,

$$\mathcal{G}_{ad} = K_{\text{ret}}(k) , \quad \mathcal{G}_{da} = K_{\text{adv}}(k) = [K_{\text{ret}}(k)]^* , \quad \mathcal{G}_{dd} = K_{\text{kel}} , \quad (5.17)$$

where K_{ret} , K_{adv} and K_{kel} denote the two-point retarded, advanced and Keldysh boundary correlators respectively.⁹ The retarded and advanced components only capture spectral information and do not depend on the occupation number n_k , as opposed to the Keldysh component that explicitly involves n_k . The absence of \mathcal{G}_{aa} follows from the Schwinger-Keldysh collapse condition. It is worth noting that the on-shell action expressed in the average-difference basis naturally produces boundary retarded correlators. The final term, \mathcal{G}_{dd} , representing the effects of fluctuations, as expected from the two-point KMS condition, is given by

$$\mathcal{G}_{dd} = \frac{1}{2} \coth \left(\frac{\beta(k^0 - \mu_q)}{2} \right) [\mathcal{G}_{ad} - \mathcal{G}_{da}] . \quad (5.18)$$

where K_{kel} denotes the two-point Keldysh boundary correlator.

With the quadratic order on-shell action established and its coefficients identified, we now focus on the quartic on-shell action $S_{(4)}$. It receives contributions from the contact diagram illustrated in Fig. 3. Using the contact term from the second line of Eq. (4.4) and considering terms up to linear order in derivatives, we obtain the following expression

$$S_{(4)} = \int d^d x \oint d\zeta \sqrt{-g} \frac{|\Phi_{(0)}|^4}{4} = \int d^d x \mathcal{L}_0 + \int d^d x \mathcal{L}_1 + \mathcal{O}((\beta\partial_t)^2) \quad (5.19)$$

where the terms \mathcal{L}_0 and \mathcal{L}_1 represent the non-derivative and first-derivative contributions to $S_{(4)}$, respectively. Note that the quartic on-shell action has been expressed in position space using Eq. (5.14). For brevity, we present only a subset of the terms in \mathcal{L}_0 and \mathcal{L}_1 here. Readers may refer to Appendix E for the complete expressions.

The explicit form of the non-derivative contribution \mathcal{L}_0 is given by

$$\mathcal{L}_0 = \sum_{r,s=0}^2 \mathcal{G}_{r,s} [\bar{J}_a]^r [J_a]^s [\bar{J}_d]^{2-r} [J_d]^{2-s} , \quad (5.20)$$

⁹The explicit expression of K_{ret} as given in Eq. (B.10).

with some of the terms described as follows

$$\mathcal{G}_{2,2} = 0 , \quad \mathcal{G}_{1,1} = 2(\zeta + \mathbb{F}_1) , \quad \mathcal{G}_{1,2} = \frac{1}{2} - \frac{\beta\mu_q}{2}(\zeta + \mathbb{F}_1) . \quad (5.21)$$

Next, we express the first-derivative contribution to the quartic on-shell action \mathcal{L}_1 as

$$\begin{aligned} \mathcal{L}_1 = & \sum_{r=0}^1 \sum_{s=0}^2 \left\{ \mathcal{G}_{\dot{r},s}(\partial_t \bar{J}_a) + \mathcal{H}_{\dot{r},s}(\partial_t \bar{J}_d) \right\} [\bar{J}_a]^r [J_a]^s [\bar{J}_d]^{1-r} [J_d]^{2-s} \\ & + \sum_{r=0}^2 \sum_{s=0}^1 \left\{ \mathcal{G}_{r,\dot{s}}(\partial_t J_a) + \mathcal{H}_{r,\dot{s}}(\partial_t J_d) \right\} [\bar{J}_a]^r [J_a]^s [\bar{J}_d]^{2-r} [J_d]^{1-s} \end{aligned} , \quad (5.22)$$

where a subset of the terms are written as

$$\begin{aligned} \mathcal{G}_{1,2} = 0 , \quad \mathcal{G}_{0,2} = \frac{i\beta}{4}(\mathbb{F}_1 - \beta\mu_q G_{1,1}^{\text{in}}) , \quad \mathcal{G}_{1,1} = \frac{i\beta}{2}(\mathbb{F}_1 - \beta\mu_q G_{1,1}^{\text{in}}) , \\ \mathcal{H}_{1,2} = -\frac{i\beta}{4}(\mathbb{F}_1 + 2\zeta + \beta\mu_q G_{1,1}^{\text{in}} - \beta\mu_q(\mathbb{F}_1 + \zeta)\mathbb{F}_2) , \end{aligned} \quad (5.23)$$

where the remaining terms are provided in Appendix E, with some of them being related to charge conjugation as outlined below:

$$\mathcal{G}_{r,s} = \mathcal{G}_{s,r} \Big|_{q \rightarrow -q} , \quad \mathcal{G}_{r,\dot{s}} = \mathcal{G}_{\dot{s},r} \Big|_{q \rightarrow -q} , \quad \mathcal{H}_{r,\dot{s}} = \mathcal{H}_{\dot{s},r} \Big|_{q \rightarrow -q} . \quad (5.24)$$

We have outlined the on-shell action (influence phase) to the leading order in the gradient expansion, highlighting the identification of several coefficients. The subsequent step is to examine how the coefficients of the quartic influence phase, are related, in a manner analogous to the quadratic case discussed in Eq. (5.18), albeit in the high-temperature limit. The next section will clarify how these relationships pave the way for the emergence of holographic non-linear FDRs at finite density under small charge expansion.

6 Holographic FDRs at finite density

In this section, we begin with the on-shell action and its coefficients, which correspond to the Schwinger-Keldysh generating functional and real-time correlators in the boundary theory. We then outline the relationships among these coefficients (i.e., the real-time correlators) and demonstrate how they lead to the fluctuation-dissipation relations (FDRs). The novelty of this work lies in the identification of non-linear relations at finite density, which we will show simplify to familiar results in the zero-density case.

We begin by quoting the 2-point KMS condition obtained above as

$$\begin{aligned} \frac{K_{\text{kel}}}{2} &= \frac{1}{4} \coth\left(\frac{\beta(k^0 - \mu_q)}{2}\right) [K_{\text{ret}} - K_{\text{adv}}] , \\ &= \frac{i}{2} \coth\left(\frac{\beta(k^0 - \mu_q)}{2}\right) \text{Im}[K_{\text{ret}}] . \end{aligned} \quad (6.1)$$

The equation above explicitly demonstrates the *linear fluctuation-dissipation relation*, as noted in [15] for zero-density holographic systems. To understand this, recall that $\text{Im}[K_{\text{ret}}]$ corresponds

to the spectral function at finite temperature, while K_{kel} represents twice the anti-commutator (refer to [34, 35] for details). Commutators present in response functions naturally measure dissipation and transport, whereas anti-commutators capture fluctuations [6]. Consequently, Eq. (6.1) provides a correct description of the linear fluctuation-dissipation relation in finite-density systems.

We now extend this study to *non-linear fluctuation-dissipation relations* at finite density by considering the quartic term in the on-shell action. To do this we note that the following relations hold at the level of $S_{(4)}$:

$$\left(\mathcal{G}_{\dot{0},0} + \mathcal{G}_{0,\dot{0}}\right) - \left(\mathcal{H}_{\dot{1},0} + \mathcal{H}_{0,\dot{1}}\right) - 2i\beta\mathcal{G}_{0,0} + \frac{i\beta}{12}(\mathcal{G}_{2,0} + \mathcal{G}_{1,1} + \mathcal{G}_{0,2}) = 0, \quad (6.2)$$

$$-\frac{1}{3}\left(\mathcal{G}_{\dot{0},2} + \mathcal{G}_{\dot{1},1} + \mathcal{G}_{2,\dot{0}} + \mathcal{G}_{1,\dot{1}}\right) + \left(\mathcal{H}_{\dot{1},2} + \mathcal{H}_{2,\dot{1}}\right) + \frac{i\beta}{3}(\mathcal{G}_{2,0} + \mathcal{G}_{1,1} + \mathcal{G}_{0,2}) = 0, \quad (6.3)$$

and

$$\begin{aligned} &-\frac{1}{3}\left(\mathcal{G}_{\dot{1},0} + \mathcal{G}_{\dot{0},1} + \mathcal{G}_{0,\dot{1}} + \mathcal{G}_{1,\dot{0}}\right) + \frac{1}{5}\left(\mathcal{H}_{\dot{0},2} + \mathcal{H}_{2,\dot{0}}\right) + \frac{2}{5}\left(\mathcal{H}_{\dot{1},1} + \mathcal{H}_{1,\dot{1}}\right) \\ &\quad - \frac{i\beta}{8}(\mathcal{G}_{1,2} + \mathcal{G}_{2,1}) + \frac{i\beta}{2}(\mathcal{G}_{0,1} + \mathcal{G}_{1,0}) = 0. \end{aligned} \quad (6.4)$$

where the terms containing time derivatives correspond to dissipation coefficients, while those without derivatives represent the fluctuation strength. Therefore, these equations describe the non-linear FDRs at finite density.

To illustrate this, we use the inverse Martin-Siggia-Rose (MSR) formalism to transform the influence phase into a stochastic field equation. Through this approach, we derive a stochastic field equation where J_a represents the stochastic field, and iJ_d corresponds to the stochastic noise. However, in this note, we focus solely on the FDRs within the effective action framework, leaving the derivation of the associated stochastic field equations for future exercise.

Zero-density limit: In the zero density limit ($\mu \rightarrow 0$), the solution (5.14) for the real scalar field χ in the gradient expansion, is given by

$$\chi = \left[J_a + \left(\zeta - \frac{1}{2} + \mathbb{F}_1 \right) J_d \right] + \frac{i\beta}{2} \left[\mathbb{F}_1 \partial_t J_a - \left(\zeta(\zeta - 1) + \left[\zeta - \frac{1}{2} \right] \mathbb{F}_1 \right) \partial_t J_d \right] + \dots, \quad (6.5)$$

and the corresponding expression of quartic on-shell action is

$$S_{(4)}^\chi = -\frac{\lambda}{4!} \oint d\zeta d^d x \sqrt{-g} \chi_{(0)}^4, \quad (6.6)$$

where superscript denotes the fact we are working with real scalar field. Evaluating the $S_{(4)}^\chi$ after doing radial contour integrals, we find

$$S_{(4)}^\chi \propto \int d^d x \left\{ \sum_{k=1}^4 \theta_k \frac{J_a^{4-k}}{(4-k)!} \frac{(iJ_d)^k}{k!} - \sum_{k=1}^3 \bar{\theta}_k \frac{J_a^{4-k}}{(4-k)!} \frac{(iJ_d)^{k-1}}{(k-1)!} \partial_t (iJ_d) \right\} \quad (6.7)$$

with the coefficients related by the following equation

$$\frac{2}{\beta} \bar{\theta}_k + \theta_{k+1} + \frac{1}{4} \theta_{k-1} = 0. \quad (6.8)$$

This is the same generalised FDRs for zero-density systems first obtained in [15], where stochastic field-theoretic description has also been developed in detail. Thus, we have reproduced the correct effective action and the non-linear FDRs in the zero density limit.

7 Discussion

In this work, we have focused on the study of (non)-linear fluctuation-dissipation relations (FDRs) for holographic systems at finite density. This was achieved by employing the RNSK geometry– the gravitational dual of the Schwinger-Keldysh formalism at finite density. While RNSK geometry has been previously studied for free fields [30], our work is the first to apply it to interacting complex scalars. We derived non-linear FDRs up to linear order in the small charge limit and reproduced the expected $q \rightarrow 0$ results. Although a complete understanding of FDRs at arbitrary charge remains a challenge, we have made notable progress in the small charge regime.

In the bulk, our approach constructs an *exterior field theory* to describe interactions in a charged black hole background, confined outside the outermost horizon. Furthermore, we extend the work of [16] by developing an exterior EFT for Hawking radiation in charged black holes. Using this theory, we developed tree-level Witten diagrammatics to compute boundary Schwinger-Keldysh correlators at finite density, providing explicit results for up to four-point functions. This diagrammatic approach can also calculate the influence phase at arbitrary orders in the coupling constant λ . Thus, it allows us to determine real-time correlators with arbitrary insertions for the holographic CFT at finite temperature and chemical potential.

There are several directions in which this investigation can be extended. A natural step forward would be to extend the analysis to systems with arbitrary values of charge. Such an extension would solidify the existence of holographic fluctuation-dissipation relations beyond zero-density systems. However, the primary challenge lies in finding solutions at an arbitrary charge, while the rest of the analysis is expected to proceed relatively smoothly.

Another interesting path involves understanding the effects of loop corrections on the exterior theory. In collaboration with R. Loganayagam and G. Martin, we have obtained preliminary results in this area, which we plan to present soon. These corrections, corresponding to $\frac{1}{N}$ effects in the boundary theory, raise important questions about how fluctuation-dissipation relations transform when such corrections are accounted for. Addressing this would help clarify the distinction between the statistical and quantum origins of fluctuations.¹⁰

Finally, a potential possibility would be to study fermionic systems and determine whether fluctuation-dissipation relations can be obtained.

Acknowledgements

I would like to thank R. Loganayagam for his advice throughout this project and Godwin Martin for many insightful discussions. I would also like to thank Subhro Bhattacharjee, Joydeep Chakravarty, Hong Liu, Gautam Mandal, Suvrat Raju, Ashoke Sen, Omkar Shetye, Akhil

¹⁰I would like to thank Hong Liu and R. Loganayagam for a discussion on this question.

Sivakumar and the ICTS string group for valuable discussions. My thanks extend to the organizers of the National Strings Meeting (NSM) 2024 at IIT Ropar and Strings 2025 at NYU Abu Dhabi, where some preliminary results of this work were presented. I would like to acknowledge the support of the Department of Atomic Energy, Government of India, under project no. RTI4001, and the unwavering and generous support provided by the people of India towards research in the fundamental sciences.

A CPT action

In this section, we will explicitly see how CPT acts on the EOM of the complex field in the RNSK geometry. As we have seen in §2, it is important for obtaining the outgoing solution from the ingoing solution. Here, we will explicitly show how mapping given in Eq. (2.6) is correct.

We begin with the field equations for a free complex scalar field Φ

$$D_M D^M \Phi = 0, \quad \text{where } D_M = \nabla_M - iq\mathcal{A}_M. \quad (\text{A.1})$$

Using the momentum space representation

$$\Phi(\zeta, v, \mathbf{x}) = \int \frac{d^d k}{(2\pi)^d} \Phi(\zeta, \omega, \mathbf{k}) e^{-i\omega v + i\mathbf{k} \cdot \mathbf{x}}, \quad (\text{A.2})$$

the field equation can be written explicitly as

$$\left\{ \left(\frac{d}{d\zeta} + \frac{\beta\omega}{2} \right) \left[r^{d-1} \left(\frac{d}{d\zeta} + \frac{\beta\omega}{2} \right) \right] - r^{d-1} \left[\left(\frac{\beta\omega}{2} \right)^2 - f \left(\frac{\beta\mathbf{k}}{2} \right)^2 \right] \right. \\ \left. + \beta q r^{d-1} \mathcal{A}_v \left(\frac{d}{d\zeta} + \frac{i\beta}{4} r f \right) \right\} \Phi_q(\zeta, \omega, \mathbf{k}) = 0 \quad (\text{A.3})$$

where we have restored the q dependence on the field. Using the substitution motivated by CPT action (2.5) in the above equation

$$\Phi_q(\zeta, \omega, \mathbf{k}) = e^{-\beta\omega\zeta - iq\Lambda} \tilde{\Phi}_q(\zeta, \omega, \mathbf{k}), \quad \text{with } \frac{d\Lambda}{d\zeta} = -i\beta\mathcal{A}_v, \quad (\text{A.4})$$

we obtain

$$\left\{ \left(\frac{d}{d\zeta} - \frac{\beta\omega}{2} - \beta q \mathcal{A}_v \right) \left[r^{d-1} \left(\frac{d}{d\zeta} - \frac{\beta\omega}{2} - \beta q \mathcal{A}_v \right) \right] - r^{d-1} \left[\left(\frac{\beta\omega}{2} \right)^2 - f \left(\frac{\beta\mathbf{k}}{2} \right)^2 \right] \right. \\ \left. + \beta q r^{d-1} \mathcal{A}_v \left(\frac{d}{d\zeta} - \beta\omega - \beta q \mathcal{A}_v + \frac{i\beta}{4} r f \right) \right\} \tilde{\Phi}_q(\zeta, \omega, \mathbf{k}) = 0 \quad (\text{A.5})$$

which when simplified, becomes

$$\left\{ \left(\frac{d}{d\zeta} - \frac{\beta\omega}{2} \right) \left[r^{d-1} \left(\frac{d}{d\zeta} - \frac{\beta\omega}{2} \right) \right] - r^{d-1} \left[\left(\frac{\beta\omega}{2} \right)^2 - f \left(\frac{\beta\mathbf{k}}{2} \right)^2 \right] \right. \\ \left. - \beta q r^{d-1} \mathcal{A}_v \left(\frac{d}{d\zeta} + \frac{i\beta}{4} r f \right) \right\} \tilde{\Phi}_q(\zeta, \omega, \mathbf{k}) = 0 \quad (\text{A.6})$$

Comparing equations (A.3) and (A.6), we can easily deduce: Given $\Phi_q(\zeta, k)$ is a solution of the EOM, the above algebraic manipulation produces another solution, given by $\tilde{\Phi}_{-q}(\zeta, -k)$. Keeping the prefactor in RHS of Eq. (A.4) in mind, we can write the ingoing-to-outgoing map in spacetimes coordinates as:

$$\Phi_q^{\text{out}}(\zeta, v, \mathbf{x}) = e^{-iq\Lambda} \Phi_{-q}^{\text{in}}(\zeta, i\beta\zeta - v, -\mathbf{x}) \quad (\text{A.7})$$

We can perform a similar analysis for the conjugate field, with the only major difference of being $q \rightarrow -q$ in the prefactor.

B Bulk-Bulk propagators in the RNSK geometry

In this section, we will discuss the derivation of bulk-to-bulk propagators for a complex field in the grSK geometry. Our derivation will closely follow the techniques used in [36, 37] and recently implemented in the grSK geometry [16].

The bulk-bulk propagator solves the following equation

$$\left\{ \left(\frac{d}{d\zeta} + \frac{\beta p^0}{2} \right) \left[r^{d-1} \left(\frac{d}{d\zeta} + \frac{\beta p^0}{2} \right) \right] - r^{d-1} \left[\left(\frac{\beta p^0}{2} \right)^2 - f \left(\frac{\beta \mathbf{p}}{2} \right)^2 \right] + \beta q r^{d-1} \mathcal{A}_v \left(\frac{d}{d\zeta} + \frac{i\beta}{4} r f \right) \right\} \mathbb{G}_q(\zeta|\zeta_0, p) = \frac{i\beta}{2} \delta(\zeta - \zeta_0), \quad (\text{B.1})$$

with the following bi-normalisable boundary conditions

$$\lim_{\zeta \rightarrow 0} \mathbb{G}_q(\zeta|\zeta_0, p) = \lim_{\zeta \rightarrow 1} \mathbb{G}_q(\zeta|\zeta_0, p) = 0. \quad (\text{B.2})$$

Using the notation used by the authors [16] and bi-normalisability of the propagator, our ansatz for the bulk-bulk propagator is

$$\mathbb{G}_q(\zeta|\zeta_0, p) = \frac{1}{W_q(\zeta_0, p)} g_L(\zeta_>, p) g_R(\zeta_<, p). \quad (\text{B.3})$$

where g_L and g_R represent boundary-bulk propagators from the left and the right boundary respectively, while W_q denotes the undetermined Wronskian. The symbols $\zeta_<$ and $\zeta_>$ are defined by

$$\zeta_{<(>)} \equiv \begin{cases} \zeta & \text{if } \zeta \text{ comes before (after) } \zeta_0 \text{ on the RNSK contour} \\ \zeta_0 & \text{if } \zeta_0 \text{ comes before (after) } \zeta \text{ on the RNSK contour.} \end{cases} \quad (\text{B.4})$$

Since the bulk-to-bulk propagator has to solve the free field equation away from the sources, it is clear that it has to be proportional to the boundary-to-bulk propagators. Left and right-normalisability then fixes this combination of the boundary-to-bulk propagators to be $g_L(\zeta_>, k) g_R(\zeta_<, k)$. The other factors in the above expression must be fixed using the jump condition coming from the delta function source in the field equation. The jump condition is obtained by integrating the Eq. (B.1), given as follows

$$\left[r^{d-1} \frac{d}{d\zeta} \mathbb{G}_q(\zeta|\zeta_0, p) \right]_{\zeta_0^-}^{\zeta_0^+} = \frac{i\beta}{2}. \quad (\text{B.5})$$

Now, we put our ansatz (B.3) into the jump condition (B.5) to obtain the Wronskian W_q as

$$\begin{aligned} W_q(\zeta, p) &= \frac{2}{i\beta} r^{d-1} \left[g_R(\zeta, p) \frac{dg_L(\zeta, p)}{d\zeta} - g_L(\zeta, p) \frac{dg_R(\zeta, p)}{d\zeta} \right] \\ &= g_L(\zeta, p) g_R^{\Pi^*}(\zeta, p) - g_R(\zeta, p) g_L^{\Pi^*}(\zeta, p) , \end{aligned} \quad (\text{B.6})$$

where we have defined left and right conjugate propagator¹¹ as

$$g_{R(L)}^{\Pi^*} \equiv -r^{d-1} \mathbb{D}_+ g_{R(L)} = -r^{d-1} \frac{2}{i\beta} \left(\frac{d}{d\zeta} + \frac{\beta p^0}{2} + \frac{\beta q}{2} \mathcal{A}_v \right) g_{R(L)} . \quad (\text{B.7})$$

Let's now apply the above differential operator to the Wronskian given above to get

$$\frac{2}{i\beta} \left(\frac{d}{d\zeta} + \beta p^0 + \beta q \mathcal{A}_v \right) W_q(\zeta, p) = g_R \mathbb{D}_+ \left[r^{d-1} \mathbb{D}_+ g_L \right] - g_L \mathbb{D}_+ \left[r^{d-1} \mathbb{D}_+ g_R \right] = 0 . \quad (\text{B.8})$$

The second equality holds upon using EOM obeyed by g_R and g_L . Hence, it implies that

$$e^{\beta p^0 \zeta + i q \wedge} W_q(\zeta, p) = \text{constant along the RNSK contour} . \quad (\text{B.9})$$

Determining the Wronskian

The retarded 2-point boundary correlator K^{in} is obtained by taking the boundary limit of the ingoing boundary-bulk conjugate propagator [21], as shown below

$$\lim_{\zeta \rightarrow 0, 1} r^{d-1} \mathbb{D}_+ G_q^{\text{in}}(\zeta, p) = \lim_{r \rightarrow \infty} r^{d-1} \mathbb{D}_+ G_q^{\text{in}}(\zeta, p) \Big|_{\text{ren}} = K_q^{\text{in}}(p) , \quad (\text{B.10})$$

where subscript ‘ren’ denotes the standard holographic renormalisation [12]. Henceforth we will stop writing this subscript as it is to be assumed in every boundary limit.

Similarly, boundary limits of the outgoing boundary-bulk conjugate propagator give

$$\begin{aligned} \lim_{\zeta \rightarrow 0} r^{d-1} \mathbb{D}_+ G_q^{\text{out}}(\zeta, p) &= \lim_{r \rightarrow \infty} r^{d-1} \mathbb{D}_+ G_{-q}^{\text{in}}(\zeta, -p) = K_{-q}^{\text{in}}(-p) , \\ \lim_{\zeta \rightarrow 1} r^{d-1} \mathbb{D}_+ G_q^{\text{out}}(\zeta, p) &= e^{-\beta(p^0 - q\mu)} \lim_{r \rightarrow \infty} r^{d-1} \mathbb{D}_+ G_{-q}^{\text{in}}(\zeta, -p) = e^{-\beta(p^0 - \mu q)} K_{-q}^{\text{in}}(-p) , \end{aligned} \quad (\text{B.11})$$

where we have used the CPT isometry: $G_q^{\text{out}}(\zeta, k) = e^{-\beta k^0 \zeta} e^{-i q \wedge} G_{-q}^{\text{in}}(\zeta, -k)$. Note that the difference between the left and right boundary limit of the outgoing conjugate propagator as opposed to the same limit of the ingoing conjugate propagator.

We now turn to the left and right conjugate propagators and their boundary limits. Using above-mentioned boundary limits, i.e. equations (B.10) and (B.11), we obtain the left boundary limits as

$$\begin{aligned} \lim_{\zeta \rightarrow 0} g_R^{\Pi^*} &\equiv - \lim_{\zeta \rightarrow 0} r^{d-1} \mathbb{D}_+ g_R = -(1 + n_p) [K_q^{\text{in}}(p) - K_{-q}^{\text{in}}(-p)] , \\ \lim_{\zeta \rightarrow 0} g_L^{\Pi^*} &\equiv - \lim_{\zeta \rightarrow 0} r^{d-1} \mathbb{D}_+ g_L = -n_p [K_q^{\text{in}}(p) - e^{\beta(p^0 - \mu q)} K_{-q}^{\text{in}}(-p)] , \end{aligned} \quad (\text{B.12})$$

¹¹By conjugate propagator, we mean the conjugate field corresponding to the propagator in question.

and the corresponding right boundary limits as

$$\begin{aligned}\lim_{\zeta \rightarrow 1} g_{\text{R}}^{\Pi^*} &\equiv -\lim_{\zeta \rightarrow 0} r^{d-1} \mathbb{D}_+ g_{\text{R}} = -(1+n_p) \left[K_{\text{q}}^{\text{in}}(p) - e^{-\beta(p^0 - \mu q)} K_{-\text{q}}^{\text{in}}(-p) \right] \\ \lim_{\zeta \rightarrow 1} g_{\text{L}}^{\Pi^*} &\equiv -\lim_{\zeta \rightarrow 0} r^{d-1} \mathbb{D}_+ g_{\text{L}} = -n_p \left[K_{\text{q}}^{\text{in}}(p) - K_{-\text{q}}^{\text{in}}(-p) \right] .\end{aligned}\tag{B.13}$$

Using these boundary limits and boundary limits of the right and the left boundary-bulk propagators Eqs. (3.13) and (3.14), we obtain the constant in eq. (B.9) at the left boundary

$$\begin{aligned}\lim_{\zeta \rightarrow 0} e^{\beta p^0 \zeta + i q \Lambda} W_{\text{q}}(\zeta, p) &= \lim_{\zeta \rightarrow 0} \left[g_{\text{L}}(\zeta, p) g_{\text{R}}^{\Pi^*}(\zeta, p) - g_{\text{R}}(\zeta, p) g_{\text{L}}^{\Pi^*}(\zeta, p) \right] \\ &= (1+n_p) \left[K_{\text{q}}^{\text{in}}(p) - K_{-\text{q}}^{\text{in}}(-p) \right] ,\end{aligned}\tag{B.14}$$

and at the right boundary also gives the same result as expected from Eq. (B.9). Since the above quantity is the same everywhere in the bulk, the expression of the Wronskian can be easily found to be

$$W_{\text{q}}(\zeta, p) = e^{-\beta p^0 \zeta - i q \Lambda} (1+n_p) \left[K_{\text{q}}^{\text{in}}(p) - K_{-\text{q}}^{\text{in}}(-p) \right] .\tag{B.15}$$

Binormalisable bulk-Bulk propagator

Now that we have expression for the Wronskian (B.15), the bi-normalisable bulk-bulk propagator (B.3) can be explicitly written as

$$\begin{aligned}\mathbb{G}_{\text{q}}(\zeta | \zeta_0, p) &= \frac{e^{\beta p^0 \zeta_0 + i q \Lambda(\zeta_0)}}{(1+n_p) \left[K_{\text{q}}^{\text{in}}(p) - K_{-\text{q}}^{\text{in}}(-p) \right]} g_{\text{L}}(\zeta_>, p) g_{\text{R}}(\zeta_<, p) \\ &= \frac{e^{\beta p^0 \zeta_0 + i q \Lambda(\zeta_0)}}{(1+n_p) \left[K_{\text{q}}^{\text{in}}(p) - K_{-\text{q}}^{\text{in}}(-p) \right]} \left\{ \Theta_{\text{SK}}(\zeta > \zeta_0) g_{\text{L}}(\zeta, p) g_{\text{R}}(\zeta_0, p) + \Theta_{\text{SK}}(\zeta < \zeta_0) g_{\text{R}}(\zeta, p) g_{\text{L}}(\zeta_0, p) \right\} .\end{aligned}\tag{B.16}$$

The bulk-bulk propagator when written ingoing-outgoing basis using the boundary-bulk propagators given in Eq. (3.12), we obtain

$$\begin{aligned}\mathbb{G}_{\text{q}}(\zeta | \zeta_0, p) &= \frac{1}{\left[K_{\text{q}}^{\text{in}}(p) - K_{-\text{q}}^{\text{in}}(-p) \right]} \\ &\times \left\{ n_p e^{\beta p^0 \zeta_0 + i q \Lambda(\zeta_0)} G_{\text{q}}^{\text{in}}(\zeta, p) G_{\text{q}}^{\text{in}}(\zeta_0, p) + (1+n_p) e^{-\beta p^0 \zeta - i q \Lambda(\zeta)} G_{-\text{q}}^{\text{in}}(\zeta, -p) G_{-\text{q}}^{\text{in}}(\zeta_0, -p) \right. \\ &\quad - \left[\Theta_{\text{SK}}(\zeta < \zeta_0) + n_p \right] G_{\text{q}}^{\text{in}}(\zeta, p) G_{-\text{q}}^{\text{in}}(\zeta_0, -p) \\ &\quad \left. - \left[\Theta_{\text{SK}}(\zeta > \zeta_0) + n_p \right] e^{\beta p^0 (\zeta_0 - \zeta)} e^{i q [\Lambda(\zeta_0) - \Lambda(\zeta)]} G_{-\text{q}}^{\text{in}}(\zeta, -p) G_{\text{q}}^{\text{in}}(\zeta_0, p) \right\} .\end{aligned}\tag{B.17}$$

As expected, it resembles the bi-normalisable bulk-bulk propagator for a real scalar field in the grSK geometry [17]. Once we have constructed the bi-normalisable propagator, we now move to retarded and advanced propagators useful in describing the causal scattering processes in the bulk. Later, we will see that they are not completely independent but related by reciprocity.

Retarded and Advanced bulk-bulk propagators

After constructing bi-normalisable bulk-bulk propagator, we can also construct bulk-to-bulk propagators that have specific causal properties, i.e., the retarded and the advanced bulk-to-bulk propagators. These propagators are normalisable at the left boundary, and analytic in the upper half and the lower half of the frequency plane respectively. Here, we will not provide a derivation of these propagators, as it is similar to the computation of the bi-normalisable bulk-to-bulk propagator given above.¹² We just quote the end results for the retarded bulk-bulk propagator

$$\begin{aligned} \mathbb{G}_{\text{ret}}(\zeta|\zeta_0, p) &= \frac{1}{[K_q^{\text{in}}(p) - K_{-q}^{\text{in}}(-p)]} \\ &\times \left\{ -e^{\beta p^0 \zeta_0 + iq\Lambda(\zeta_0)} G_q^{\text{in}}(\zeta, p) G_q^{\text{in}}(\zeta_0, p) + \Theta_{\text{SK}}(\zeta > \zeta_0) G_q^{\text{in}}(\zeta, p) G_{-q}^{\text{in}}(\zeta_0, -p) \right. \\ &\quad \left. + \Theta_{\text{SK}}(\zeta < \zeta_0) e^{\beta p^0 (\zeta_0 - \zeta)} e^{iq[\Lambda(\zeta_0) - \Lambda(\zeta)]} G_{-q}^{\text{in}}(\zeta, -p) G_q^{\text{in}}(\zeta_0, p) \right\} \end{aligned} \quad (\text{B.18})$$

and the advanced bulk-bulk propagator

$$\begin{aligned} \mathbb{G}_{\text{adv}}(\zeta|\zeta_0, p) &= \frac{1}{[K_q^{\text{in}}(p) - K_{-q}^{\text{in}}(-p)]} \\ &\times \left\{ e^{-\beta p^0 \zeta - iq\Lambda(\zeta)} G_{-q}^{\text{in}}(\zeta, -p) G_{-q}^{\text{in}}(\zeta_0, -p) - \Theta_{\text{SK}}(\zeta < \zeta_0) G_q^{\text{in}}(\zeta, p) G_{-q}^{\text{in}}(\zeta_0, -p) \right. \\ &\quad \left. - \Theta_{\text{SK}}(\zeta > \zeta_0) e^{\beta p^0 (\zeta_0 - \zeta)} e^{iq[\Lambda(\zeta_0) - \Lambda(\zeta)]} G_{-q}^{\text{in}}(\zeta, -p) G_q^{\text{in}}(\zeta_0, p) \right\} \end{aligned} \quad (\text{B.19})$$

Note that we have suppressed the label q for the retarded and advanced propagators.

The reciprocity relation of the bi-normalisable bulk-bulk propagator can be easily found from the Eq. (B.17) as follows

$$\mathbb{G}_q(\zeta|\zeta_0, p) = \mathbb{G}_{-q}(\zeta_0|\zeta, -p) \equiv \bar{\mathbb{G}}_q(\zeta_0|\zeta, -p) , \quad (\text{B.20})$$

where we have defined the bar as an action which changes the sign of charge: $q \mapsto -q$.

The bi-normalisable bulk-bulk propagator can be written as a linear combination of retarded and advanced bulk-bulk propagators given as

$$\mathbb{G}(\zeta|\zeta_0, p) = -n_p \mathbb{G}_{\text{ret}}(\zeta|\zeta_0, p) + (1 + n_p) \mathbb{G}_{\text{adv}}(\zeta|\zeta_0, p) , \quad (\text{B.21})$$

and then the reciprocity at the level of retarded and advanced propagators is given by

$$\mathbb{G}_{\text{adv}}(\zeta|\zeta_0, p) = \bar{\mathbb{G}}_{\text{ret}}(\zeta_0|\zeta, -p) . \quad (\text{B.22})$$

¹²Again, readers are encouraged to look at [17] for detailed analysis.

C Discontinuities on the RNSK geometry

In this section, we examine the integration over the RNSK geometry, relevant to the on-shell action calculation. Specifically, the calculation involves a contour integral over the complexified radius, as depicted in Fig. (1). This integral can be simplified into a single exterior integral, defined in Eq. (4.16), with the discontinuities arising from the horizon cap. Here, we will outline these discontinuities and demonstrate how they are computed.

The discontinuity arises due to the non-analytic nature of the integrand, which originate from the outgoing propagators. These non-analyticities are introduced through terms such as ζ and Λ . Notably, $e^{-iq\Lambda}$ experiences a jump by $e^{\beta\mu q}$ across contour branches, and ζ increments by unity. These factors collectively explain the origin of the discontinuity.

To understand this, consider the following integral

$$\oint_{\zeta} \left[e^{\beta\mu q - iq\Lambda(\zeta)} \right]^{\alpha} \prod_{i=1}^{\alpha} e^{\beta k_i^0 (1-\zeta)} \mathcal{F}(\zeta) = \frac{-1}{n_{\alpha, \sum k_i}} \int_{\text{ext}} \left[e^{-iq\Lambda(\zeta)} \right]^{\alpha} \prod_{i=1}^{\alpha} e^{-\beta k_i^0 \zeta} \mathcal{F}(\zeta), \quad (\text{C.1})$$

where $\mathcal{F}(\zeta)$ is an analytic function and recall the definition of \int_{ext} and n

$$\int_{\text{ext}} \equiv \int_{r_h}^{r_c} dr r^{d-1}, \quad n_{\alpha, k} = \frac{1}{e^{\beta(k^0 - \alpha\mu q)} - 1}. \quad (\text{C.2})$$

This is the only type of discontinuity that arises in a single integral, representing the most general form of a single discontinuity. It can be explicitly verified that this result yields the correct expressions for contact diagrams. However, as we move beyond contact diagrams—for example, to exchange diagrams—a greater number of bulk integrals appear, often accompanied by multiple bulk-to-bulk propagators. Therefore, it becomes necessary to extend this result to multi-discontinuities, starting with double discontinuities.

To declutter the expressions in more complicated integrals, we find it convenient to define Θ as

$$\Theta \equiv -\frac{1}{\mu} \int_0^{\zeta} d\zeta' \mathcal{A}_v(\zeta') = \int_0^{\zeta} d\zeta' \left(\frac{r_{\pm}}{r} \right)^{d-2} \quad \text{or} \quad \Lambda = i\beta\mu\Theta, \quad (\text{C.3})$$

where we note that the Θ jumps by unity across the horizon cap.

Now we will come to the computation of exchange diagrams that contain bulk-to-bulk propagators. The simplest exchange diagrams consist of double integrals over the RNSK contour. The most general form of such an integral is

$$\begin{aligned} \oint_{\zeta_1, \zeta_2} \prod_{i=1}^2 e^{-\beta\mu q \alpha_i [1-\Theta(\zeta_i)]} e^{\beta\kappa_i (1-\zeta_i)} \mathcal{F}(\zeta_1, \zeta_2) \mathbb{G}(\zeta_2 | \zeta_1, p) \\ = \int_{\text{ext}} \prod_{i=1}^2 e^{-\beta\mu q \alpha_i [1-\Theta(\zeta_i)]} e^{\beta\kappa_i (1-\zeta_i)} \mathcal{F}(\zeta_1, \zeta_2) \mathbb{G}_{\text{dd}}(\zeta_2 | \zeta_1, p), \end{aligned} \quad (\text{C.4})$$

where $\mathcal{F}(\zeta)$ is again an analytic function and the the double-discontinuity \mathbb{G}_{dd} is given by

$$\begin{aligned} \mathbb{G}_{\text{dd}}(\zeta_2 | \zeta_1, p) \equiv & \mathbb{G}(\zeta_2 | \zeta_1, p) - e^{\beta(\mu q \alpha_1 - \kappa_1)} \mathbb{G}(\zeta_2 | \zeta_1 + 1, p) \\ & - e^{\beta(\mu q \alpha_2 - \kappa_2)} \mathbb{G}(\zeta_2 + 1 | \zeta_1, p) + e^{\beta(\mu q \alpha_1 + \mu q \alpha_2 - \kappa_1 - \kappa_2)} \mathbb{G}(\zeta_2 + 1 | \zeta_1 + 1, p). \end{aligned} \quad (\text{C.5})$$

The exponential factors in the above expression are simply the monodromy factors due to the branch cut extending from the horizon radius r_+ to the cut-off radius r_c on the complex r plane. We can now use the expression for the bulk-to-bulk propagator given in Eq.(A.33) to evaluate the integrand above explicitly. We will use the theta function identities. Using the following properties of step functions on the grSK contour

$$\Theta_{\text{SK}}(\zeta + 1 > \zeta' + 1) = \Theta_{\text{SK}}(\zeta < \zeta') , \quad (\text{C.6})$$

and

$$\Theta_{\text{SK}}(\zeta + 1 > \zeta') = 1 , \quad \Theta_{\text{SK}}(\zeta > \zeta' + 1) = 0 , \quad (\text{C.7})$$

where $\zeta, \zeta' < \zeta_h$ or both ζ and ζ' are on the left exterior contour.

Substituting the expressions for bulk-bulk propagator from Eq. (B.19), the double-discontinuity obtained is as follows

$$\mathbb{G}_{\text{dd}}(\zeta|\zeta', p) = \frac{-n_{1,p}}{(1+n_{\alpha_1-1, \kappa_1-1})(1+n_{\alpha_2, \kappa_2})} \mathbb{G}_{\text{ret}}(\zeta|\zeta', p) + \frac{(1+n_{1,p})}{(1+n_{\alpha_1, \kappa_1})(1+n_{\alpha_2+1, \kappa_2+p})} \mathbb{G}_{\text{adv}}(\zeta|\zeta', p) . \quad (\text{C.8})$$

We observe that the double-discontinuity formula reduces to the result in [16] in the $q \rightarrow 0$ limit. Though a generalization to multi-discontinuities is possible, we focus on the double-discontinuity in this work.

D On-shell action for $|\Phi|^4$ theory

In this section, we present the on-shell action for the $|\Phi|^4$ theory using a method introduced in [17]. This approach circumvents the need to evaluate the boundary terms in the on-shell action explicitly. It leverages the fact that the boundary value of the higher-order solution vanishes, thereby simplifying the computation.

The bare action is given by

$$S_{\text{bare}} = - \oint d^{d+1}x \sqrt{-g} \left(|D_M \Phi|^2 + \frac{\lambda}{2!2!} (\bar{\Phi}\Phi)^2 \right) . \quad (\text{D.1})$$

Inserting the perturbative solution into the bare action yields the on-shell action in the following form.

$$S_{\text{os}} = - \int_{\partial\mathcal{M}} d\Sigma^A \Phi_{(0)} \overline{(D_A \Phi_{(0)})} + \lambda \oint_{\mathcal{M}} \left[\frac{1}{2!} (\bar{\Phi} - \bar{\Phi}_{(0)}) \Phi (\bar{\Phi}\Phi) - \frac{1}{2!2!} (\bar{\Phi}\Phi)^2 \right] , \quad (\text{D.2})$$

where we have used the equations of motion and imposed the appropriate boundary conditions to significantly simplify the expression for the on-shell action. When expanded in terms of the coupling constant, the on-shell action is explicitly expressed as follows:

$$\begin{aligned} S_{(2)} &= - \int_{\partial\mathcal{M}} d\Sigma^A \Phi_{(0)} \overline{(D_A \Phi_{(0)})} , \\ S_{(4)} &= - \frac{\lambda}{2!2!} \oint d^{d+1}x \sqrt{-g} (\bar{\Phi}_{(0)} \Phi_{(0)})^2 , \\ S_{(6)} &= - \frac{\lambda^2}{2} \oint d^{d+1}x \sqrt{-g} \bar{\Phi}_{(0)} \Phi_{(1)} \bar{\Phi}_{(0)} \Phi_{(0)} , \end{aligned} \quad (\text{D.3})$$

where the above terms represent both free and contact contributions at the tree level in Feynman diagrams.

We find it convenient to express the on-shell action in the Past-Future (PF) basis, i.e. Eqs. (3.8) and (3.17). In this basis, SK collapse (unitarity) and KMS condition (thermality) are reflected in the vanishing of coefficients of all F s and the P s terms respectively. Moreover, this basis exclusively involves retarded/advanced propagators in the correlators, ensuring the description of causal scattering processes.

Now, we turn to explicit calculation of on-shell action, starting from the contact term $S_{(4)}$ of the $|\Phi|^4$ theory.

Contact term: The contact term $S_{(4)}$ is given in the second line of the eq. (4.4). Passing into the boundary momentum variables, it can be written as

$$\begin{aligned}
S_{(4)} &= -\frac{\lambda}{4} \int_{k_{1,2,3,4}} \oint_{\zeta} \prod_{i=1}^2 \bar{\Phi}_{(0)}(\zeta, k_i) \prod_{j=1}^2 \Phi_{(0)}(\zeta, k_j) \\
&= -\frac{\lambda}{4} \int_{k_{1,2,3,4}} \oint_{\zeta} \prod_{i=1}^2 \left\{ -\bar{G}^{\text{in}}(\zeta, k_i) \bar{J}_{\bar{F}}(k_i) + e^{\beta(k_i^0 + \mu q)} \bar{G}^{\text{out}}(\zeta, k_i) \bar{J}_{\bar{F}}(k_i) \right\} \\
&\quad \times \prod_{j=1}^2 \left\{ -G^{\text{in}}(\zeta, k_j) J_{\bar{F}}(k_j) + e^{\beta(k_j^0 - \mu q)} G^{\text{out}}(\zeta, k_j) J_{\bar{F}}(k_j) \right\}
\end{aligned} \tag{D.4}$$

where we have written the solution in terms of ingoing and outgoing solution, as given in eq. (3.6) and eq. (3.15).

Taking into account the analyticity of G^{in} and \bar{G}^{in} in the ζ coordinate and using momentum conservation, the RNSK radial integral leads us to the following observations:

1. SK collapse holds: The term with only $\bar{J}_{\bar{F}}$ and $J_{\bar{F}}$ vanishes.
2. KMS condition holds: The term with only $\bar{J}_{\bar{F}}$ and $J_{\bar{F}}$ vanishes.

As a result, seven of the original nine terms remain. The next step involves performing the RNSK integral to obtain a single exterior integral, using the eq. (C.1) from the previous appendix. Thus,

we obtain

$$\begin{aligned}
S_{(4)} = & -\lambda \int_{k_{1,2,3,4}} \int_{\text{ext}} \left\{ \frac{1}{2n_{1,k_4}} \bar{J}_{\bar{F}}(k_1) J_{\bar{F}}(k_2) \bar{J}_{\bar{F}}(k_3) J_{\bar{F}}(k_4) \bar{G}^{\text{in}}(\zeta, k_1) G^{\text{in}}(\zeta, k_2) \bar{G}^{\text{in}}(\zeta, k_3) G^{\text{out}}(\zeta, k_4) \right. \\
& + \frac{1}{2\bar{n}_{1,k_3}} \bar{J}_{\bar{F}}(k_1) J_{\bar{F}}(k_2) \bar{J}_{\bar{F}}(k_3) J_{\bar{F}}(k_4) \bar{G}^{\text{in}}(\zeta, k_1) G^{\text{in}}(\zeta, k_2) \bar{G}^{\text{out}}(\zeta, k_3) G^{\text{in}}(\zeta, k_4) \\
& - \frac{1}{n_{0,k_{34}}} \bar{J}_{\bar{F}}(k_1) J_{\bar{F}}(k_2) \bar{J}_{\bar{F}}(k_3) J_{\bar{F}}(k_4) \bar{G}^{\text{in}}(\zeta, k_1) G^{\text{in}}(\zeta, k_2) \bar{G}^{\text{out}}(\zeta, k_3) G^{\text{out}}(\zeta, k_4) \\
& - \frac{1}{n_{2,k_{24}}} \bar{J}_{\bar{F}}(k_1) J_{\bar{F}}(k_2) \bar{J}_{\bar{F}}(k_3) J_{\bar{F}}(k_4) \bar{G}^{\text{in}}(\zeta, k_1) G^{\text{out}}(\zeta, k_2) \bar{G}^{\text{in}}(\zeta, k_3) G^{\text{out}}(\zeta, k_4) \\
& - \frac{1}{\bar{n}_{2,k_{13}}} \bar{J}_{\bar{F}}(k_1) J_{\bar{F}}(k_2) \bar{J}_{\bar{F}}(k_3) J_{\bar{F}}(k_4) \bar{G}^{\text{out}}(\zeta, k_1) G^{\text{in}}(\zeta, k_2) \bar{G}^{\text{out}}(\zeta, k_3) G^{\text{in}}(\zeta, k_4) \\
& + \frac{1}{2n_{1,k_{234}}} \bar{J}_{\bar{F}}(k_1) J_{\bar{F}}(k_2) \bar{J}_{\bar{F}}(k_3) J_{\bar{F}}(k_4) \bar{G}^{\text{in}}(\zeta, k_1) G^{\text{out}}(\zeta, k_2) \bar{G}^{\text{out}}(\zeta, k_3) G^{\text{out}}(\zeta, k_4) \\
& \left. + \frac{1}{2\bar{n}_{1,k_{134}}} \bar{J}_{\bar{F}}(k_1) J_{\bar{F}}(k_2) \bar{J}_{\bar{F}}(k_3) J_{\bar{F}}(k_4) \bar{G}^{\text{out}}(\zeta, k_1) G^{\text{in}}(\zeta, k_2) \bar{G}^{\text{out}}(\zeta, k_3) G^{\text{out}}(\zeta, k_4) \right\}, \tag{D.5}
\end{aligned}$$

as noted previously, these exterior integrals naturally exhibit Bose-Einstein factors. These seven terms correspond to the seven diagrams shown in Figure (3).

Exchange terms: Having addressed the contact term, the next step is to examine the exchange terms. In the case of $|\Phi|^4$ theory, the first exchange term originate from the six-point influence phase $S_{(6)}$, which appears at quadratic order in λ . The $S_{(6)}$ is given in the third line of eq. (4.4) and is expressed in momentum space as

$$S_{(6)} = -\frac{\lambda^2}{2} \int_{k_{1,2,3,4}} \oint_{\zeta, \zeta'} \bar{\Phi}_{(0)}(\zeta, k_1) \Phi_{(0)}(\zeta, k_2) \bar{\Phi}_{(0)}(\zeta, k_3) \mathbb{G}(\zeta|\zeta', k_4) \mathcal{J}_{(1)}(\zeta', k_4). \tag{D.6}$$

Upon using the expression of bulk source $\mathcal{J}_{(1)}$ from eq. (3.30), we find

$$\begin{aligned}
S_{(6)} = & -\frac{\lambda^2}{4} \int_{k_{1,2,\dots,6}} \oint_{\zeta, \zeta'} \\
& \times \bar{\Phi}_{(0)}(\zeta, k_1) \Phi_{(0)}(\zeta, k_2) \bar{\Phi}_{(0)}(\zeta, k_3) \mathbb{G}(\zeta|\zeta', k_{456}) \Phi_{(0)}(\zeta', k_4) \bar{\Phi}_{(0)}(\zeta', k_5) \Phi_{(0)}(\zeta', k_6). \tag{D.7}
\end{aligned}$$

Using the expressions of zeroth-order solution equations (3.6), (3.15) and (B.17), we get

$$\begin{aligned}
S_{(6)} = & -\frac{\lambda^2}{4} \int_{k_{1,2,\dots,6}} \oint_{\zeta, \zeta'} \left[-\bar{G}^{\text{in}}(\zeta, k_1) \bar{J}_{\bar{F}}(k_1) + e^{\beta(k_1^0 + \mu q)} \bar{G}^{\text{out}}(\zeta, k_1) \bar{J}_{\bar{F}}(k_1) \right] \\
& \times \left[-G^{\text{in}}(\zeta, k_2) J_{\bar{F}}(k_2) + e^{\beta(k_2^0 - \mu q)} G^{\text{out}}(\zeta, k_2) J_{\bar{F}}(k_2) \right] \left[-\bar{G}^{\text{in}}(\zeta, k_3) \bar{J}_{\bar{F}}(k_3) + e^{\beta(k_3^0 + \mu q)} \bar{G}^{\text{out}}(\zeta, k_3) \bar{J}_{\bar{F}}(k_3) \right] \\
& \times \mathbb{G}(\zeta|\zeta', k_{456}) \left[-G^{\text{in}}(\zeta, k_4) J_{\bar{F}}(k_4) + e^{\beta(k_4^0 - \mu q)} G^{\text{out}}(\zeta, k_4) J_{\bar{F}}(k_4) \right] \\
& \times \left[-\bar{G}^{\text{in}}(\zeta, k_5) \bar{J}_{\bar{F}}(k_5) + e^{\beta(k_5^0 + \mu q)} \bar{G}^{\text{out}}(\zeta, k_5) \bar{J}_{\bar{F}}(k_5) \right] \left[-G^{\text{in}}(\zeta, k_6) J_{\bar{F}}(k_6) + e^{\beta(k_6^0 - \mu q)} G^{\text{out}}(\zeta, k_6) J_{\bar{F}}(k_6) \right]. \tag{D.8}
\end{aligned}$$

Once again, the SK collapse and KMS condition are evident, as all F s and P s terms vanish in the six-point influence phase $S_{(6)}$.

We proceed with the RNSK integral to express $S_{(6)}$ in terms of the exterior radial integrals. Here, we present the result for a single term of $S_{(6)}$, specifically the component with five F s and one P s, denoted as $S_{5\bar{F},1\bar{P}}$. This term comprises two independent contributions, as shown below

$$S_{5\bar{F},1\bar{P}} = S[\bar{F}\bar{F}\bar{F}\bar{F}\bar{P}] + S[\bar{F}\bar{F}\bar{F}\bar{P}\bar{F}], \quad (\text{D.9})$$

where the notation is designed to clearly indicate whether the past source is from the field or its conjugate. Now, let us analyze the case where the past source is from the field, written as

$$S[\bar{F}\bar{F}\bar{F}\bar{F}\bar{P}] = \frac{\lambda^2}{4} \int_{k_{1,2,\dots,6}} \bar{J}_{\bar{F}}(k_1) J_{\bar{F}}(k_2) \bar{J}_{\bar{F}}(k_3) J_{\bar{F}}(k_4) \bar{J}_{\bar{F}}(k_5) J_{\bar{F}}(k_6) \oint_{\zeta, \zeta'} \mathbb{G}(\zeta|\zeta', k_{456}) \times \left[\bar{G}^{\text{in}}(\zeta, k_1) G^{\text{in}}(\zeta, k_2) \bar{G}^{\text{in}}(\zeta, k_3) G^{\text{in}}(\zeta', k_4) \bar{G}^{\text{in}}(\zeta', k_5) e^{\beta(k_6^0 - \mu q)} G^{\text{out}}(\zeta', k_6) \right]. \quad (\text{D.10})$$

Using double-discontinuity integral given in the eq. (C.4) from the previous Appendix, we find

$$S[\bar{F}\bar{F}\bar{F}\bar{F}\bar{P}] = \frac{\lambda^2}{2} \int_{k_{1,2,\dots,6}} \frac{1}{n_{1,k_6}} \bar{J}_{\bar{F}}(k_1) J_{\bar{F}}(k_2) \bar{J}_{\bar{F}}(k_3) J_{\bar{F}}(k_4) \bar{J}_{\bar{F}}(k_5) J_{\bar{F}}(k_6) \times \int_{\text{ext}} \mathbb{G}_{\text{ret}}(\zeta|\zeta', k_{456}) \left[\bar{G}^{\text{in}}(\zeta, k_1) G^{\text{in}}(\zeta, k_2) \bar{G}^{\text{in}}(\zeta, k_3) G^{\text{in}}(\zeta', k_4) \bar{G}^{\text{in}}(\zeta', k_5) G^{\text{out}}(\zeta', k_6) \right]. \quad (\text{D.11})$$

It is worth emphasizing that the result above was derived by leveraging the reciprocity between the retarded and advanced bulk-bulk propagators.

Similarly, one could extend this approach to compute additional terms in the six-point influence phase. However, since the same principles apply, we restrict our focus to a single term in this appendix. By employing a similar analysis and multi-discontinuity integrals, exchange terms contributing to the higher-order influence phase can also be determined.

E Explicit terms of quartic on-shell action $S_{(4)}$

In this section, we will explicitly compute the four-point influence phase at linear order in the gradient expansion. In time domain, we start with the solution itself

$$\Phi = \left[J_a + \left(\zeta - \frac{1}{2} + \mathbb{F}_1 \right) J_d \right] + \frac{i\beta}{2} \left[\mathbb{F}_1 \partial_t J_a - \left(\zeta(\zeta - 1) + \left[\zeta - \frac{1}{2} \right] \mathbb{F}_1 \right) \partial_t J_d \right] + \frac{\beta\mu q}{2} \left[(\mathbb{F}_2 - \mathbb{F}_1) J_a + \left(\zeta(\zeta - 1) + \left[\zeta - \frac{1}{2} \right] \mathbb{F}_2 + \left(\zeta - \frac{1}{2} + \mathbb{F}_2 \right) \mathbb{F}_1 \right) J_d \right]. \quad (\text{E.1})$$

Since we are only working up to linear order in derivatives, we can divide the following terms into two parts:

$$\int d^d x \oint d\zeta \sqrt{-g} \frac{|\Phi|^4}{4} = \int d^d x \mathcal{L}_0 + \int d^d x \mathcal{L}_1 + \mathcal{O}((\beta\partial_t)^2) \quad (\text{E.2})$$

where \mathcal{L}_0 and \mathcal{L}_1 are non-derivative and first derivative term.

As we can see now, we can make our lives easier by moving into position space. It will remove unnecessary notation and declutter the expressions.

Zeroth-derivative term \mathcal{L}_0 : The \mathcal{L}_0 can be explicitly written as

$$\mathcal{L}_0 = \sum_{r,s=0}^2 \mathcal{G}_{r,s} [\bar{J}_a]^r [J_a]^s [\bar{J}_d]^{2-r} [J_d]^{2-s} . \quad (\text{E.3})$$

where some of the terms are as follows

$$\begin{aligned} \mathcal{G}_{2,2} &= 0 , & \mathcal{G}_{1,1} &= 2(\zeta + \mathbb{F}_1) , & \mathcal{G}_{1,2} &= \frac{1}{2} - \frac{\beta\mu_q}{2}(\zeta + \mathbb{F}_1) , \\ \mathcal{G}_{2,1} &= \frac{1}{2} + \frac{\beta\mu_q}{2}(\zeta + \mathbb{F}_1) , & \mathcal{G}_{0,0} &= \frac{1}{4}(\zeta + \mathbb{F}_1) + (\zeta + \mathbb{F}_1)^3 , \\ \mathcal{G}_{0,2} &= \frac{1}{2}(\zeta + \mathbb{F}_1) - \frac{3\beta\mu_q}{4}(\zeta + \mathbb{F}_1)^2 , & \mathcal{G}_{2,0} &= \frac{1}{2}(\zeta + \mathbb{F}_1) + \frac{3\beta\mu_q}{4}(\zeta + \mathbb{F}_1)^2 , \\ \mathcal{G}_{0,1} &= \frac{1}{8} + \frac{3}{2}(\zeta + \mathbb{F}_1)^2 - \frac{\beta\mu_q}{8}(\zeta + \mathbb{F}_1) - \beta\mu_q(\zeta + \mathbb{F}_1)^3 , \\ \mathcal{G}_{1,0} &= \frac{1}{8} + \frac{3}{2}(\zeta + \mathbb{F}_1)^2 + \frac{\beta\mu_q}{8}(\zeta + \mathbb{F}_1) + \beta\mu_q(\zeta + \mathbb{F}_1)^3 . \end{aligned} \quad (\text{E.4})$$

Note that the following is true

$$\mathcal{G}_{r,s} = \mathcal{G}_{s,r} \Big|_{q \rightarrow -q} , \quad (\text{E.5})$$

Note that the above statement is quite general as will see later.

First-derivative term \mathcal{L}_1 : In the first derivative term, the time derivative can appear on any of the four sources. Thus, we can explicitly write \mathcal{L}_1 as

$$\begin{aligned} \mathcal{L}_1 &= \sum_{r=0}^1 \sum_{s=0}^2 \mathcal{G}_{\dot{r},s} (\partial_t \bar{J}_a) [\bar{J}_a]^r [J_a]^s [\bar{J}_d]^{1-r} [J_d]^{2-s} + \sum_{r=0}^2 \sum_{s=0}^1 \mathcal{G}_{r,\dot{s}} (\partial_t J_a) [\bar{J}_a]^r [J_a]^s [\bar{J}_d]^{2-r} [J_d]^{1-s} \\ &+ \sum_{r=0}^1 \sum_{s=0}^2 \mathcal{H}_{\dot{r},s} (\partial_t \bar{J}_d) [\bar{J}_a]^r [J_a]^s [\bar{J}_d]^{1-r} [J_d]^{2-s} + \sum_{r=0}^2 \sum_{s=0}^1 \mathcal{H}_{r,\dot{s}} (\partial_t J_d) [\bar{J}_a]^r [J_a]^s [\bar{J}_d]^{2-r} [J_d]^{1-s} \end{aligned} \quad (\text{E.6})$$

which in concise form

$$\begin{aligned} \mathcal{L}_1 &= \sum_{r=0}^1 \sum_{s=0}^2 \left\{ \mathcal{G}_{\dot{r},s} (\partial_t \bar{J}_a) + \mathcal{H}_{\dot{r},s} (\partial_t \bar{J}_d) \right\} [\bar{J}_a]^r [J_a]^s [\bar{J}_d]^{1-r} [J_d]^{2-s} \\ &+ \sum_{r=0}^2 \sum_{s=0}^1 \left\{ \mathcal{G}_{r,\dot{s}} (\partial_t J_a) + \mathcal{H}_{r,\dot{s}} (\partial_t J_d) \right\} [\bar{J}_a]^r [J_a]^s [\bar{J}_d]^{2-r} [J_d]^{1-s} \end{aligned} \quad (\text{E.7})$$

where some of the terms are as follows

$$\begin{aligned} \mathcal{G}_{1,2} &= 0 , & \mathcal{G}_{\dot{0},2} &= \frac{i\beta}{4}(\mathbb{F}_1 - \beta\mu_q G_{1,1}^{\text{in}}) , & \mathcal{G}_{1,1} &= \frac{i\beta}{2}(\mathbb{F}_1 - \beta\mu_q G_{1,1}^{\text{in}}) , \\ \mathcal{G}_{1,0} &= \frac{i\beta}{2}(\mathbb{F}_1 - \beta\mu_q G_{1,1}^{\text{in}})(\mathbb{F}_1 + \zeta) , & \mathcal{G}_{\dot{0},1} &= i\beta(\mathbb{F}_1 - \beta\mu_q G_{1,1}^{\text{in}})(\mathbb{F}_1 + \zeta) , \\ \mathcal{G}_{\dot{0},0} &= \frac{i\beta}{4}(\mathbb{F}_1 - \beta\mu_q G_{1,1}^{\text{in}}) \left(\frac{1}{4} + 3(\mathbb{F}_1 + \zeta)^2 \right) . \end{aligned} \quad (\text{E.8})$$

Again, we notice that the following holds

$$\mathcal{G}_{r,\dot{s}} = \mathcal{G}_{\dot{s},r} \Big|_{q \rightarrow -q} , \quad \mathcal{H}_{r,\dot{s}} = \mathcal{H}_{\dot{s},r} \Big|_{q \rightarrow -q} . \quad (\text{E.9})$$

Now, we turn to the terms involving \dot{J}_d and they are explicitly given as

$$\begin{aligned}
\mathcal{H}_{i,2} &= -\frac{i\beta}{4} \left(\mathbb{F}_1 + 2\zeta + \beta\mu_q G_{1,1}^{\text{in}} - \beta\mu_q (\mathbb{F}_1 + \zeta) \mathbb{F}_2 \right), \\
\mathcal{H}_{0,2} &= \frac{i\beta}{8} \left\{ -2(\mathbb{F}_1 + \zeta)(\mathbb{F}_1 + 3\zeta) + \beta(-2G_{1,1}^{\text{in}}(\mathbb{F}_1 + 2\zeta) + \mathbb{F}_2(2\mathbb{F}_1^2 + 6\mathbb{F}_1\zeta + 3\zeta^2))\mu_q + \mathbb{F}_2\beta\mu_q G_{2,0}^{\text{in}} - 2\beta\mu_q G_{2,1}^{\text{in}} \right\}, \\
\mathcal{H}_{i,1} &= \frac{i\beta}{4} \left\{ -2(\mathbb{F}_1 + \zeta)(\mathbb{F}_1 + 3\zeta) + \beta(-2G_{1,1}^{\text{in}}(\mathbb{F}_1 + 2\zeta) + \mathbb{F}_2(2\mathbb{F}_1^2 + 6\mathbb{F}_1\zeta + 3\zeta^2))\mu_q + \mathbb{F}_2\beta\mu_q G_{2,0}^{\text{in}} - 2\beta\mu_q G_{2,1}^{\text{in}} \right\}, \\
\mathcal{H}_{0,1} &= \frac{i\beta}{8} \left\{ (-\mathbb{F}_1 - 4\mathbb{F}_1^3 - 2\zeta - 24\mathbb{F}_1^2\zeta - 36\mathbb{F}_1\zeta^2 - 16\zeta^3 - \beta\mu_q G_{1,1}^{\text{in}} + \beta(\mathbb{F}_1 + \zeta)(\mathbb{F}_2 - 4G_{1,1}^{\text{in}}(\mathbb{F}_1 + 3\zeta) \right. \\
&\quad \left. + 4\mathbb{F}_2(\mathbb{F}_1^2 + 4\mathbb{F}_1\zeta + 2\zeta^2))\mu_q) + \beta(\mathbb{F}_1 + \zeta)\mu_q(\mathbb{F}_2 G_{2,0}^{\text{in}} - 2G_{2,1}^{\text{in}}) \right\}, \\
\mathcal{H}_{i,0} &= \frac{i\beta}{16} \left\{ (-\mathbb{F}_1 - 4\mathbb{F}_1^3 - 2\zeta - 24\mathbb{F}_1^2\zeta - 36\mathbb{F}_1\zeta^2 - 16\zeta^3 - \beta\mu_q G_{1,1}^{\text{in}} + \beta(\mathbb{F}_1 + \zeta)(\mathbb{F}_2 - 4G_{1,1}^{\text{in}}(\mathbb{F}_1 + 3\zeta) \right. \\
&\quad \left. + 4\mathbb{F}_2(\mathbb{F}_1^2 + 4\mathbb{F}_1\zeta + 2\zeta^2))\mu_q) + \beta(\mathbb{F}_1 + \zeta)\mu_q(\mathbb{F}_2 G_{2,0}^{\text{in}} - 2G_{2,1}^{\text{in}}) \right\}, \\
\mathcal{H}_{0,0} &= \frac{i\beta}{32} \left\{ -2(\mathbb{F}_1 + \zeta)(3\mathbb{F}_1 + 4\mathbb{F}_1^3 + 7\zeta + 28\mathbb{F}_1^2\zeta + 44\mathbb{F}_1\zeta^2 + 20\zeta^3) + \beta\mu_q(1 + 12(\mathbb{F}_1 + \zeta)^2)(\mathbb{F}_2 G_{2,0}^{\text{in}} - 2G_{2,1}^{\text{in}}) \right. \\
&\quad \left. + \beta\mu_q \left\{ (2\mathbb{F}_1(3 + 4\mathbb{F}_1^2)(-G_{1,1}^{\text{in}} + \mathbb{F}_1\mathbb{F}_2) + 2(-4G_{1,1}^{\text{in}}(1 + 6\mathbb{F}_1^2) + 7\mathbb{F}_1(1 + 4\mathbb{F}_1^2)\mathbb{F}_2)\zeta \right. \right. \\
&\quad \left. \left. + (7\mathbb{F}_2 + 36\mathbb{F}_1(-2G_{1,1}^{\text{in}} + 3\mathbb{F}_1\mathbb{F}_2))\zeta^2 + 16(-2G_{1,1}^{\text{in}} + 5\mathbb{F}_1\mathbb{F}_2)\zeta^3 + 20\mathbb{F}_2\zeta^4 \right\} \right\}.
\end{aligned} \tag{E.10}$$

References

- [1] R. Kubo, *The fluctuation-dissipation theorem*, *Rept. Prog. Phys.* **29** (1966), no. 1 255.
- [2] R. Kubo, *Statistical mechanical theory of irreversible processes. 1. General theory and simple applications in magnetic and conduction problems*, *J. Phys. Soc. Jap.* **12** (1957) 570–586.
- [3] P. C. Martin and J. S. Schwinger, *Theory of many particle systems. 1.*, *Phys. Rev.* **115** (1959) 1342–1373.
- [4] E. Wang and U. Heinz, *Generalized fluctuation-dissipation theorem for nonlinear response functions*, *Phys. Rev. D* **66** (Jul, 2002) 025008.
- [5] N. Tsuji, T. Shitara, and M. Ueda, *Out-of-time-order fluctuation-dissipation theorem*, *Phys. Rev. E* **97** (2018), no. 1 012101, [[arXiv:1612.08781](#)].
- [6] F. M. Haehl, R. Loganayagam, P. Narayan, A. A. Nizami, and M. Rangamani, *Thermal out-of-time-order correlators, KMS relations, and spectral functions*, *JHEP* **12** (2017) 154, [[arXiv:1706.08956](#)].
- [7] B. Chakrabarty, S. Chaudhuri, and R. Loganayagam, *Out of Time Ordered Quantum Dissipation*, *JHEP* **07** (2019) 102, [[arXiv:1811.01513](#)].
- [8] B. Chakrabarty and S. Chaudhuri, *Out of time ordered effective dynamics of a quartic oscillator*, *SciPost Phys.* **7** (2019) 013, [[arXiv:1905.08307](#)].
- [9] B. Chakrabarty, J. Chakravarty, S. Chaudhuri, C. Jana, R. Loganayagam, and A. Sivakumar, *Nonlinear Langevin dynamics via holography*, *JHEP* **01** (2020) 165, [[arXiv:1906.07762](#)].

- [10] D. T. Son and A. O. Starinets, *Minkowski space correlators in AdS / CFT correspondence: Recipe and applications*, *JHEP* **09** (2002) 042, [[hep-th/0205051](#)].
- [11] D. T. Son and D. Teaney, *Thermal Noise and Stochastic Strings in AdS/CFT*, *JHEP* **07** (2009) 021, [[arXiv:0901.2338](#)].
- [12] K. Skenderis and B. C. van Rees, *Real-time gauge/gravity duality*, *Phys. Rev. Lett.* **101** (2008) 081601, [[arXiv:0805.0150](#)].
- [13] K. Skenderis and B. C. van Rees, *Real-time gauge/gravity duality: Prescription, Renormalization and Examples*, *JHEP* **05** (2009) 085, [[arXiv:0812.2909](#)].
- [14] P. Glorioso, M. Crossley, and H. Liu, *A prescription for holographic Schwinger-Keldysh contour in non-equilibrium systems*, [arXiv:1812.08785](#).
- [15] C. Jana, R. Loganayagam, and M. Rangamani, *Open quantum systems and Schwinger-Keldysh holograms*, *JHEP* **07** (2020) 242, [[arXiv:2004.02888](#)].
- [16] R. Loganayagam and G. Martin, *An Exterior EFT for Hawking Radiation*, [arXiv:2403.10654](#).
- [17] G. Martin and S. K. Sharma, *Open EFT for Interacting Fermions from Holography*, [arXiv:2403.10604](#).
- [18] F. M. Haehl and M. Rangamani, *Records from the S-Matrix Marathon: Schwinger-Keldysh Formalism*, 10, 2024. [arXiv:2410.10602](#).
- [19] R. Loganayagam, K. Ray, and A. Sivakumar, *Fermionic Open EFT from Holography*, [arXiv:2011.07039](#).
- [20] S. Colin-Ellerin, X. Dong, D. Marolf, M. Rangamani, and Z. Wang, *Real-time gravitational replicas: Formalism and a variational principle*, *JHEP* **05** (2021) 117, [[arXiv:2012.00828](#)].
- [21] J. K. Ghosh, R. Loganayagam, S. G. Prabhu, M. Rangamani, A. Sivakumar, and V. Vishal, *Effective field theory of stochastic diffusion from gravity*, *JHEP* **05** (2021) 130, [[arXiv:2012.03999](#)].
- [22] Y. Bu, T. Demircik, and M. Lublinsky, *All order effective action for charge diffusion from Schwinger-Keldysh holography*, *JHEP* **05** (2021) 187, [[arXiv:2012.08362](#)].
- [23] T. He, R. Loganayagam, M. Rangamani, and J. Virrueta, *An effective description of momentum diffusion in a charged plasma from holography*, *JHEP* **01** (2022) 145, [[arXiv:2108.03244](#)].
- [24] Y. Bu and B. Zhang, *Schwinger-Keldysh effective action for a relativistic Brownian particle in the AdS/CFT correspondence*, *Phys. Rev. D* **104** (2021), no. 8 086002, [[arXiv:2108.10060](#)].
- [25] T. He, R. Loganayagam, M. Rangamani, A. Sivakumar, and J. Virrueta, *The timbre of Hawking gravitons: an effective description of energy transport from holography*, *JHEP* **09** (2022) 092, [[arXiv:2202.04079](#)].
- [26] T. He, R. Loganayagam, M. Rangamani, and J. Virrueta, *An effective description of charge diffusion and energy transport in a charged plasma from holography*, *JHEP* **03** (2023) 161, [[arXiv:2205.03415](#)].
- [27] R. Loganayagam, M. Rangamani, and J. Virrueta, *Holographic open quantum systems: toy models and analytic properties of thermal correlators*, *JHEP* **03** (2023) 153, [[arXiv:2211.07683](#)].
- [28] C. Pantelidou and B. Withers, *Thermal three-point functions from holographic Schwinger-Keldysh contours*, *JHEP* **04** (2023) 050, [[arXiv:2211.09140](#)].
- [29] S. Caron-Huot, *Holographic cameras: an eye for the bulk*, *JHEP* **03** (2023) 047,

[[arXiv:2211.11791](#)].

- [30] R. Loganayagam, K. Ray, S. K. Sharma, and A. Sivakumar, *Holographic KMS relations at finite density*, *JHEP* **03** (2021) 233, [[arXiv:2011.08173](#)].
- [31] B. Chakrabarty and A. P. M., *Open effective theory of scalar field in rotating plasma*, *JHEP* **08** (2021) 169, [[arXiv:2011.13223](#)].
- [32] A. Sivakumar, *Real Time Correlations and Complexified Horizons*, [arXiv:2410.18188](#).
- [33] S. A. Hartnoll, A. Lucas, and S. Sachdev, *Holographic quantum matter*, [arXiv:1612.07324](#).
- [34] A. Kamenev, *Field Theory of Non-Equilibrium Systems*. Cambridge University Press, 2011.
- [35] S. Chaudhuri, C. Chowdhury, and R. Loganayagam, *Spectral Representation of Thermal OTO Correlators*, *JHEP* **02** (2019) 018, [[arXiv:1810.03118](#)].
- [36] P. Arnold and D. Vaman, *4-point correlators in finite-temperature AdS/CFT: Jet quenching correlations*, *JHEP* **11** (2011) 033, [[arXiv:1109.0040](#)].
- [37] T. Faulkner, N. Iqbal, H. Liu, J. McGreevy, and D. Vegh, *Charge transport by holographic Fermi surfaces*, *Phys. Rev. D* **88** (2013) 045016, [[arXiv:1306.6396](#)].